






## ARTICLE

# Active PI3K abrogates central tolerance in high-avidity autoreactive B cells

Sarah A. Greaves<sup>1</sup>, Jacob N. Peterson<sup>1</sup>, Pamela Strauch<sup>1</sup>, Raul M. Torres<sup>1,2</sup>, and Roberta Pelanda<sup>1,2</sup>

**Autoreactive B cells that bind self-antigen with high avidity in the bone marrow undergo mechanisms of central tolerance that prevent their entry into the peripheral B cell population. These mechanisms are breached in many autoimmune patients, increasing their risk of B cell-mediated autoimmune diseases. Resolving the molecular pathways that can break central B cell tolerance could therefore provide avenues to diminish autoimmunity. Here, we show that B cell-intrinsic expression of a constitutively active form of PI3K-P110 $\alpha$  by high-avidity autoreactive B cells of mice completely abrogates central B cell tolerance and further promotes these cells to escape from the bone marrow, differentiate in peripheral tissue, and undergo activation in response to self-antigen. Upon stimulation with T cell help factors, these B cells secrete antibodies in vitro but remain unable to secrete autoantibodies in vivo. Overall, our data demonstrate that activation of the PI3K pathway leads high-avidity autoreactive B cells to breach central, but not late, stages of peripheral tolerance.**

## Introduction

Mechanisms of B cell tolerance have evolved to reduce the autoreactive capacity of the immune system and the chance of developing autoimmunity. The large numbers of autoreactive B cells that are generated daily in the bone marrow (Grandien et al., 1994; Wardemann et al., 2003) are negatively selected via three distinct processes of central B cell tolerance: anergy, receptor editing, and clonal deletion. During central tolerance, immature B cells with B cell antigen receptors (BCRs) that bind self-antigen with a low-avidity exit the bone marrow but are rendered anergic and unable to contribute to immune responses (reviewed in Cambier et al., 2007; Goodnow et al., 2010). In contrast, B cells with BCRs that bind self-antigen with higher avidity undergo receptor editing, a process during which immature B cells continue to rearrange their Ig light chain genes to form a new BCR (Nemazee, 2006; Pelanda and Torres, 2006; Lang et al., 2016). To reinforce central tolerance, autoreactive B cells that undergo editing but fail to produce non-autoreactive antigen receptors undergo clonal deletion (Halverson et al., 2004; Pelanda and Torres, 2012).

To exit the bone marrow and enter the peripheral B cell compartment, immature B cells must generate a “tonic” signal downstream of a nonautoreactive (ligand independent), or a slightly autoreactive, BCR (Bannish et al., 2001; Tze et al., 2005; Wen et al., 2005). This tonic signal is crucial for the bone marrow export of newly generated B cells, their differentiation into transitional and mature cell stages, and their long-term

survival in the periphery (Lam et al., 1997; Loder et al., 1999; Kouskoff et al., 2000; Kraus et al., 2004; Pelanda and Torres, 2012). The specific biochemical pathways that regulate BCR tonic signaling have yet to be fully elucidated. Elucidation of these pathways is important, because their activation in autoreactive cells could skew central B cell selection toward enhanced generation of autoreactive cells, a phenomenon observed in many patients afflicted by autoimmune disorders (Samuels et al., 2005; Yurasov et al., 2005; Kinnunen et al., 2013; Tipton et al., 2015). The signaling mediators rat sarcoma (RAS), ERK, and phosphoinositide 3-kinase (PI3K), which encompass small GTPases, MAP kinases, and lipid kinases, respectively, are involved in many fundamental cellular processes in all cell types, including B cells (Okkenhaug and Vanhaesebroeck, 2003; Rajalingam et al., 2007; Roskoski, 2012). By using mouse models of central B cell tolerance, we have previously shown that basal activation of both RAS and ERK is higher in bone marrow nonautoreactive immature B cells compared with autoreactive cells (Rowland et al., 2010a; Teodorovic et al., 2014). Moreover, bone marrow culture studies with pharmacologic inhibitors have indicated that both active ERK and PI3K are required for the differentiation of nonautoreactive immature B cells to the transitional stage (Teodorovic et al., 2014). Furthermore, introduction of the constitutively active form of NRAS, NRASD12, in autoreactive immature B cells leads to partial break of central

<sup>1</sup>Department of Immunology and Microbiology, University of Colorado School of Medicine, Anschutz Medical Campus, Aurora, CO; <sup>2</sup>Department of Biomedical Research, National Jewish Health, Denver, CO.

Correspondence to Roberta Pelanda: [roberta.pelanda@ucdenver.edu](mailto:roberta.pelanda@ucdenver.edu).

© 2019 Greaves et al. This article is distributed under the terms of an Attribution–Noncommercial–Share Alike–No Mirror Sites license for the first six months after the publication date (see <http://www.rupress.org/terms/>). After six months it is available under a Creative Commons License (Attribution–Noncommercial–Share Alike 4.0 International license, as described at <https://creativecommons.org/licenses/by-nc-sa/4.0/>).

tolerance via a process requiring both the ERK and PI3K signaling cascades (Teodorovic et al., 2014). However, when we studied mice with a constitutively active form of mitogen-activated protein kinase kinase 1 (MEK1) in B cells, we were surprised to find that the specific activation of the MEK-ERK pathway does not prevent, or even alter, central B cell tolerance (Greaves et al., 2018). These observations suggest that the PI3K pathway might be more relevant in this context.

Class IA PI3Ks, the PI3Ks relevant to B cells, are membrane-associated kinases that, upon activation, produce the phospholipid phosphatidylinositol-(3,4,5)-trisphosphate (PIP3). In turn, PIP3 activates several downstream mediators (e.g., protein kinase B, also known as AKT, and Tec-family tyrosine kinases) that trigger an array of essential cellular processes, including cell survival, proliferation, and metabolic fitness (Okkenhaug and Vanhaesebroeck, 2003; Baracho et al., 2011; Okkenhaug, 2013). B cells express significant amounts of the class IA isoforms PI3K $\alpha$  and PI3K $\delta$ , which play a redundant function during B cell development, regulating RAG1/2 expression, IL-7 responses, and B cell maturation (Ramadani et al., 2010; Baracho et al., 2011; Okkenhaug, 2013). PI3K $\delta$  plays a more unique role in mature B cells, contributing to cell survival and cell activation in response to antigen (Okkenhaug et al., 2002; Ramadani et al., 2010; Okkenhaug, 2013; So et al., 2013). Nevertheless, a constitutively active form of PI3K $\alpha$  (P110\*; Klippel et al., 1996) was shown to function in mature B cells by sustaining their survival after BCR deletion (Srinivasan et al., 2009). In the context of B cell tolerance, activation of the PI3K pathway achieved via the deletion of its negative regulators phosphatase and tensin homolog (PTEN) or Src homology 2 domain containing inositol polyphosphate 5-phosphatase 1 (SHIP-1) has been shown to sustain the survival and activation of low-avidity (anergic) autoreactive B cells (Browne et al., 2009; Getahun et al., 2016). Of interest, gain-of-function mutations in PI3K have been described in humans, and a third of these patients display autoimmune manifestations including production of autoantibodies (Coulter et al., 2017). Moreover, recent studies have described the immune system of mice bearing the most common PI3K $\delta$  gain-of-function mutation found in humans. These mice recapitulate many of the key immune dysfunctions observed in patients, including B cell lymphopenia and increased autoantibodies (Avery et al., 2018; Preite et al., 2018; Wray-Dutra et al., 2018). However, the role PI3K plays in central B cell tolerance is much less understood. Supraphysiological RAG expression and secondary Ig gene recombination events have been observed in nonautoreactive Ig transgenic immature B cells that lack PI3K activity in the presence or absence of BCR engagement (Llorian et al., 2007; Verkoczy et al., 2007), suggesting that PI3K may play a role in receptor editing. In addition, PTEN-deficient immature B cells are more resistant to apoptosis induced by IgM crosslinking, suggesting that PI3K activation may be able to protect autoreactive B cells from clonal deletion (Cheng et al., 2009; Gonzalez-Martin et al., 2016). Nonetheless, whether activation of PI3K is sufficient to terminate receptor editing in autoreactive immature B cells undergoing central B cell tolerance and promote their differentiation and export into the periphery has not been established.

To test these questions, we used the Rosa26-P110\* mouse strain (Srinivasan et al., 2009) and the mb1Cre mouse strain (Hobeika et al., 2006) to express a synthetic constitutively active form of PI3K $\alpha$  (P110\*; Klippel et al., 1996) in B cells of Ig heavy (H) and light (L) chain 3-83 knock-in mice, with or without the related high-avidity self-antigen MHC-I H-2K<sup>b</sup> (Pelanda et al., 1997; Braun et al., 2000; Halverson et al., 2004). Using this approach, we show that increasing the activation of the PI3K pathway in high-avidity autoreactive B cells, to levels observed in nonautoreactive cells, leads to the complete inhibition of receptor editing in the bone marrow, the continued maturation and egress of autoreactive B cells to the periphery, and their activation in response to self-antigen.

## Results

### PI3K-AKT activity is higher in nonautoreactive than autoreactive immature B cells

It has been shown that BCR ligation of bone marrow IgM<sup>+</sup> immature B cells decreases the amount of cellular PIP3 (Verkoczy et al., 2005), suggesting the activity of PI3K is reduced in developing B cells that bind self-antigens relative to those that do not. The PIP3 lipid is required to target AKT to the plasma membrane, where it becomes phosphorylated and thereby activated (Manning and Toker, 2017). Thus, AKT phosphorylation is often used as a surrogate for PI3K activation. To interrogate at the single-cell level whether the activity of PI3K is lower in autoreactive than nonautoreactive immature B cells, we used flow cytometry to compare the amount of phosphorylated AKT (pAKT) in B220<sup>+</sup>IgD<sup>-</sup> cells from the bone marrow of 3-83Igi, H-2<sup>b</sup> and 3-83Igi, H-2<sup>d</sup> mice (Fig. 1 A; Pelanda et al., 1997; Braun et al., 2000; Halverson et al., 2004). Developing B cells in these mice express the 3-83 (H+K) BCR, which has high avidity for the self-antigen MHC-I H-2K<sup>b</sup> but does not react with H-2K<sup>d</sup> (Nemazee and Bürki, 1989; Lang et al., 1996). Due to the presence of pre-arranged Ig 3-83 H and L chain genes, moreover, developing 3-83Igi B cells bypass the small pre-B cell stage and are mostly (~90%) B220<sup>+</sup>IgD<sup>-</sup> immature B cells expressing the 3-83 IgM BCR (Braun et al., 2000; Halverson et al., 2004). Phosphorylation of AKT S473, which is mediated by target of rapamycin (mTOR) complex 2 (mTORC2) to maximize and stabilize AKT activity (Limon and Fruman, 2012; Manning and Toker, 2017), was detected at similar levels in autoreactive and nonautoreactive cells (Fig. 1, A and B). In contrast, the phosphorylation of AKT T308, which is mediated by 3-phosphoinositide-dependent protein kinase 1 and is necessary for (and correlating with) AKT function (Limon and Fruman, 2012; Manning and Toker, 2017), was twice as high in nonautoreactive relative to autoreactive cells (Fig. 1, B and C). These findings indicate that the activity of the PI3K-AKT pathway is higher in nonautoreactive than autoreactive immature B cells.

### Development of mice with active PI3K in autoreactive and nonautoreactive B cells

We next developed a mouse model with which to investigate in vivo whether PI3K activation can alter the establishment of central B cell tolerance (Fig. 2 A). To achieve this, we crossed

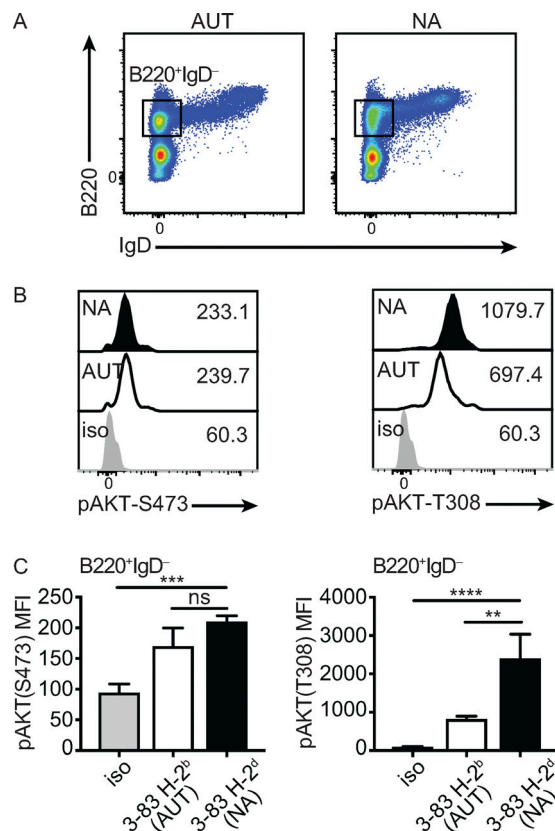


**Figure 1. PI3K activity in autoreactive and nonautoreactive immature B cells.** (A) Example of gating B220<sup>+</sup>IgD<sup>-</sup> immature B cells within the bone marrow cell population of 3-83Igi, H-2<sup>b</sup> autoreactive (AUT) and 3-83Igi, H-2<sup>d</sup> nonautoreactive (NA) mice. (B) Representative pAKT flow analysis at residues S473 (left) and T308 (right) in B220<sup>+</sup>IgD<sup>-</sup> bone marrow cells of autoreactive and nonautoreactive mice, gated as in A. The staining isotype (iso) controls are shown in gray. Numbers next to histograms indicate the MFI of each sample. (C) Average amounts of pAKT-S473 (left) and pAKT-T308 (right), displayed as MFI ± SEM, measured in bone marrow immature (B220<sup>+</sup>IgD<sup>-</sup>) B cells of autoreactive (white bars) and nonautoreactive (black bars) mice, as shown in B. The gray bars represent the isotype controls (n = 6). Data in all panels are representative of n = 6–8 mice per group analyzed over five independent experiments. P values were calculated using a one-tailed Mann-Whitney U test. \*\*, P ≤ 0.01; \*\*\*, P ≤ 0.001; \*\*\*\*, P ≤ 0.0001; ns, not significant.

3-83Igi autoreactive (H-2<sup>b</sup>) or nonautoreactive (H-2<sup>d</sup>) mice to mb1Cre, a mouse strain in which expression of Cre recombinase is restricted to the B cell lineage (Hobeika et al., 2006). We then bred 3-83Igi, mb1Cre mice to Rosa26-P110\* mice (Srinivasan et al., 2009), whose B cells, in the presence of the Cre enzyme, coexpress GFP and P110\*, a constitutively active synthetic form of PI3K-P110α (Klippel et al., 1996). Thus, these mice allow us to determine the effects of active PI3Kα on the selection of either nonautoreactive or high-avidity autoreactive immature B cells (Fig. 2 A). To validate this mouse strain, we analyzed by flow cytometry in both B cells and non-B cells the expression of GFP, which represents P110\*. Expression of GFP was generally limited to B cells, as denoted by its detection in >90% of B220<sup>+</sup> cells and <1% of B220<sup>-</sup> cells in both the bone marrow and spleen of 3-83Igi P110\*-mb1Cre mice (Fig. 2 B).

To further establish the functionality of the P110\* allele in developing B cells, we examined the amount of pAKT-T308

in B220<sup>+</sup>IgD<sup>-</sup> bone marrow cells of autoreactive and nonautoreactive 3-83Igi P110\*-mb1Cre mice (henceforth referred to as P110\*) relative to mb1Cre littermate controls. The expression of P110\* increased the average amount of pAKT-T308 by twofold in autoreactive immature B cells (Fig. 2 C, left), reaching levels measured in nonautoreactive cells (Figs. 1 B and 2 C, right). This increase was not observed in non-B cells (Fig. S1 A), further validating the B cell-restricted expression of P110\*. Interestingly, phospho-AKT-T308 was only slightly increased in nonautoreactive cells expressing P110\* (Fig. 2 C, right), possibly suggesting the presence of a negative feedback loop that prevents excessive AKT activity. We have previously shown that phosphorylated ERK (pERK) is also approximately twofold higher in (untreated) nonautoreactive immature B cells relative to autoreactive cells and that ERK activity is required for the in vitro differentiation of immature B cells into transitional B cells (Teodorovic et al., 2014). Surprisingly, the expression of P110\* also led to significantly higher amounts of pERK in autoreactive immature B cells (Fig. 2 D).

Overall, these data demonstrate that autoreactive B cells from 3-83Igi, H-2<sup>b</sup> mb1Cre-P110\* mice express the PI3Kα constitutively active form P110\*, which leads to enhanced phosphorylation of AKT and ERK to levels displayed by nonautoreactive cells.

### B cell-intrinsic activation of PI3K leads to diminished B cell development but increased numbers of CD21<sup>+</sup> transitional B cells in the bone marrow

Before analyzing parameters of central B cell tolerance, we characterized the general phenotype of bone marrow B cells in P110\* relative to control mice. The number of B220<sup>+</sup> cells was significantly decreased in the bone marrow of autoreactive and nonautoreactive P110\* mice (Fig. 3 A), an observation consistent with findings in mice bearing B cells deficient for SHIP, a negative regulator of PI3K (Liu et al., 1998; Leung et al., 2013). To compare the distribution of B cell subsets, bone marrow B cells were gated as described in Fig. 3 (B and C). Because GFP<sup>+</sup> cells were rare in B220<sup>+</sup> CD24<sup>-</sup> and/or CD21<sup>-</sup> cells (Fig. S1 B), these latter cells (which are mostly Hardy's fraction A pro-B cells; Hardy et al., 2012) were excluded from the analyses. The numbers of B220<sup>+</sup>CD24<sup>hi</sup>CD2<sup>-</sup> pro-B cells were similar with or without P110\* and regardless of autoreactivity (Fig. 3 D). However, the numbers of B220<sup>+</sup>CD24<sup>hi</sup>CD2<sup>+</sup> immature B-to-transitional B cells and B220<sup>+</sup>CD24<sup>hi</sup>CD21<sup>-</sup>CD23<sup>-</sup> pro-B-to-immature B cells were significantly diminished, greater than threefold in P110\* mice, whether autoreactive or nonautoreactive (Fig. 3 D). The diminished numbers of developing B cells in P110\* mice were associated with a reduced expression of IL-7R/CD127 (Fig. S1, C and D), a receptor known to be negatively regulated by the PI3K-AKT pathway (Lazorchak et al., 2010; Shojaee et al., 2016).

Immature B cells can first differentiate within the bone marrow into transitional CD21<sup>+</sup>CD23<sup>-</sup> T1-like and CD21<sup>+</sup>CD23<sup>+</sup> T2-like cells before their export to the periphery (Lindsley et al., 2007; Rowland et al., 2010b). When we measured these markers, we observed a sizeable fraction of the CD24<sup>hi</sup> B cell population of P110\* autoreactive mice shifting to a more transitional T1-like phenotype (Fig. 3, C and D). This was further accompanied by elevated CR2/CD21 gene transcripts (Fig. S1 E). Generation of



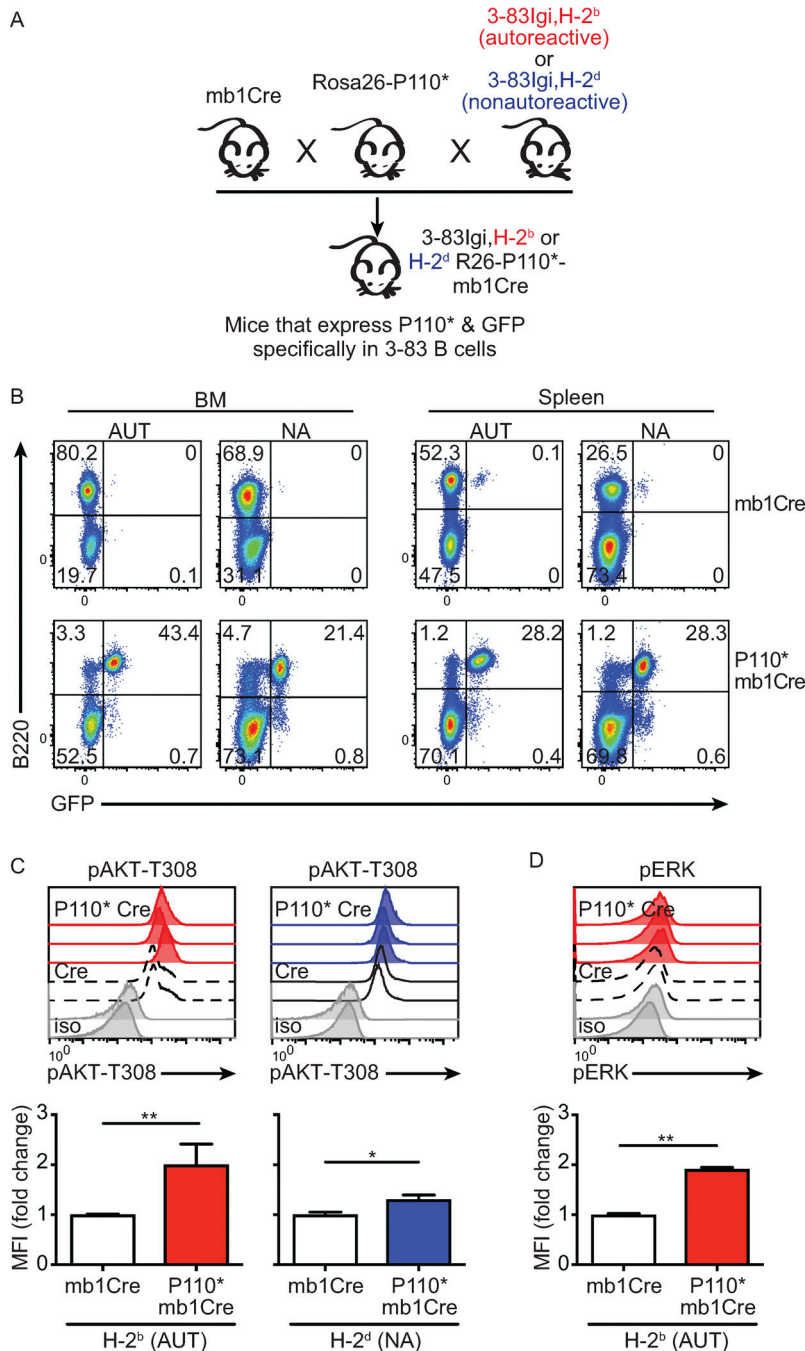


**Figure 2. Development of mouse models with increased PI3K activity in autoreactive and nonautoreactive B cells.** **(A)** Schematic for the generation of 3-83Igi mouse models of tolerance with P110\* and GFP coexpression in autoreactive or nonautoreactive B cells. **(B)** Expression of B220 and GFP by bone marrow (BM) and spleen lymphocytes of autoreactive (AUT; 3-83Igi,H-2<sup>b</sup>) and nonautoreactive (NA; 3-83Igi,H-2<sup>d</sup>) mice carrying the mb1Cre allele with or without the P110\* allele. Numbers are frequencies of cells in each quadrant. Data are representative of at least four experiments and nine mice per each group. **(C)** Top: pAKT-T308 flow analyses of B220<sup>+</sup>IgD<sup>-</sup> bone marrow cells (gated as in Fig. 1A) isolated from autoreactive 3-83Igi,H-2<sup>b</sup> mb1Cre mice with (red shaded) or without (black dashed line) P110\* (left) and nonautoreactive 3-83Igi,H-2<sup>d</sup> mb1Cre mice with (blue shaded) or without (black intact line) P110\* (right) analyzed in one experiment. The staining isotype (iso) controls are shown in gray. Each histogram represents a mouse. Data are representative of at least two experiments. Bottom: Bar graphs show the average fold change of pAKT-T308 in B220<sup>+</sup>IgD<sup>-</sup> bone marrow cells of P110\* mice relative to their mb1Cre controls. The individual MFI fold changes were calculated dividing the MFI of each individual mouse by the average MFI of mb1Cre mice in the same experiment. Data shown represent the mean ± SEM from *n* = 8 and 4 autoreactive mice with mb1Cre and P110\*-mb1Cre, respectively, analyzed in three independent experiments, and *n* = 5 and 4 nonautoreactive mice with mb1Cre and P110\*-mb1Cre, respectively, analyzed in two independent experiments. **(D)** pERK flow analysis of B220<sup>+</sup>IgD<sup>-</sup> bone marrow cells isolated from autoreactive mb1Cre mice with (red shaded histograms and red bars) or without (black dashed line and white bars) P110\*. Data shown represent the mean ± SEM from *n* = 8 mb1Cre and *n* = 4 P110\*-mb1Cre mice analyzed in three independent experiments. P values were calculated using a one-tailed Mann-Whitney *U* test. \*, *P* ≤ 0.05; \*\*, *P* ≤ 0.01.

CD21<sup>+</sup> T1-like B cells was also increased in P110\* nonautoreactive mice, but to a much lesser extent than in autoreactive animals (Fig. 3 D). In contrast, the numbers of both CD24<sup>hi</sup>CD23<sup>+</sup> T2-like cells and CD24<sup>low</sup>CD23<sup>+</sup> recirculating mature B cells were decreased in all P110\* mice regardless of autoreactivity (Fig. 3 D). To specifically address whether the PI3K pathway is required for the generation of transitional B cells, we analyzed the development of CD21<sup>+</sup> and IgD<sup>+</sup> cells in bone marrow B cell cultures (Rowland et al., 2010a,b). Treatment of nonautoreactive immature B cell cultures with the PI3K inhibitor LY294002 led to significantly lower frequencies of both CD21<sup>+</sup> and IgD<sup>+</sup> transitional B cells (Fig. S2 A). Interestingly, treatment of cultures with rapamycin, which inhibits the PI3K downstream pathway

mTORC1, did not reduce and instead augmented the development of transitional B cells (Fig. S2 A), though both inhibitors affected the phosphorylation of ribosomal protein S6 (Fig. S2 B).

These data indicate that activation of PI3K reduces the overall production of immature B cells independently of self-reactivity but leads to CD21 up-regulation and the generation of transitional B cells via a process that does not require mTORC1.

**Activation of PI3K leads to the complete inhibition of receptor editing in developing autoreactive B cells in vivo**

Elegant studies have demonstrated that PI3K is a crucial regulator of RAG1 and RAG2 expression during B cell development (Llorian et al., 2007; Verkoczy et al., 2007; Amin and Schlissel,

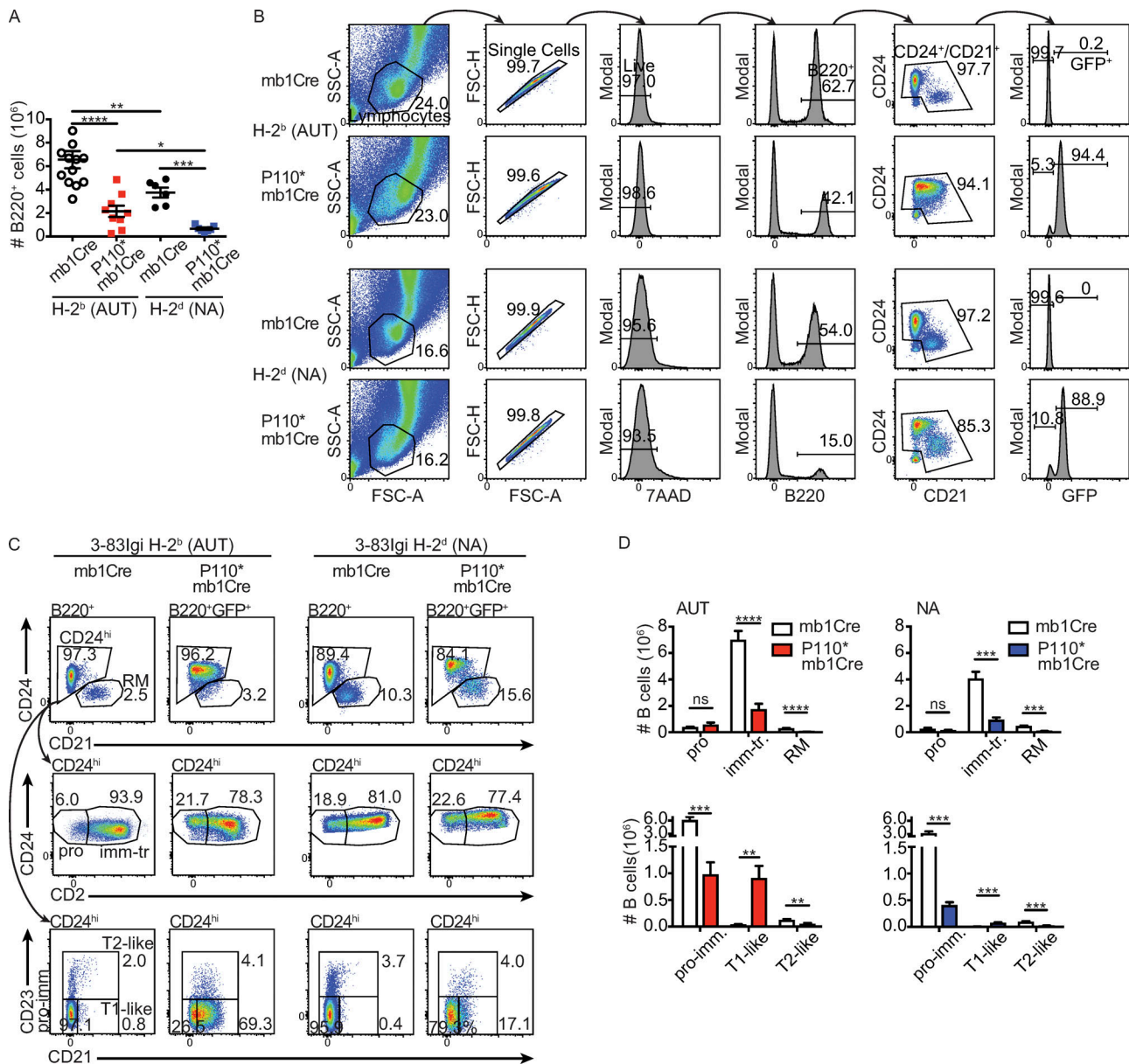


**Figure 3. Activation of PI3K leads to reduced B cell development but increased numbers of CD21<sup>+</sup> B cells.** (A) Absolute numbers of B220<sup>+</sup> cells (gated as in Fig. 3 B) in bone marrow of autoreactive 3–83Igi, H-2<sup>b</sup> (AUT; *n* = 9–13 per group analyzed in five experiments) and nonautoreactive 3–83Igi, H-2<sup>d</sup> (NA; *n* = 6–7 per group analyzed in three experiments) mice with either mb1Cre (circles) or P110\*–mb1Cre (squares). B220<sup>+</sup> cells from P110\*–mb1Cre mice were additionally gated on GFP<sup>+</sup>. Data show the mean ± SEM and were analyzed using a one-tailed Mann–Whitney *U* test. (B) Serial gating strategy for the analysis of bone marrow B cells from 3–83Igi autoreactive and nonautoreactive mice with or without P110\*. B220<sup>+</sup>CD24<sup>hi</sup>CD21<sup>+</sup> cells, which are fraction A pro–B cells, were excluded from the analyses because they included few GFP<sup>+</sup> cells in P110\* mice (Fig. S1 B). Data are representative of at least four experiments and 6–13 mice per group. (C and D) Gating strategy (C) and average numbers (D) of pro–B cells (B220<sup>+</sup>CD24<sup>hi</sup>CD21<sup>+</sup>, pro), immature-transitional B cells (B220<sup>+</sup>CD24<sup>hi</sup>CD21<sup>+</sup>, imm-tr), recirculating mature B cells (B220<sup>+</sup>CD24<sup>lo</sup>CD21<sup>+</sup>, RM), pro–B-immature B cells (B220<sup>+</sup>CD24<sup>hi</sup>CD21<sup>+</sup>CD23<sup>+</sup>, pro-imm), T1-like B cells (B220<sup>+</sup>CD24<sup>hi</sup>CD21<sup>+</sup>CD23<sup>+</sup>), and T2-like B cells (B220<sup>+</sup>CD24<sup>hi</sup>CD21<sup>+</sup>CD23<sup>+</sup>) in bone marrow from autoreactive and nonautoreactive caP110\*–mb1Cre and mb1Cre control mice. B220<sup>+</sup> and B220<sup>+</sup>GFP<sup>+</sup> cells in the top panels in C were gated as shown in Fig. 3 B. Numbers in flow plots are frequencies of each subset. *n* = 10–13 for Cre and *n* = 8–9 for P110\* autoreactive mice (analyzed in five experiments), and *n* = 6 for Cre and *n* = 7 for P110\* nonautoreactive mice (analyzed in four experiments) in bar graphs (D). Results shown represent the mean ± SEM and were analyzed using a one-tailed unpaired *t* test. \*\*, *P* ≤ 0.01; \*\*\*, *P* ≤ 0.001; \*\*\*\*, *P* ≤ 0.0001; ns, not significant. 7AAD, 7-aminoactinomycin D; FSC-H, forward scatter height; FSC-A, forward scatter area; SSC-A, side scatter area.

2008; Dengler et al., 2008; Herzog et al., 2008; Ramadani et al., 2010). However, whether PI3K activation can overcome antigen-induced BCR signaling in autoreactive B cells to terminate receptor editing, a process also relying on RAGs, has not been determined.

Autoreactive B cells undergoing editing express little or no membrane IgM due to antigen-mediated receptor internalization (Pelanda et al., 1997). In contrast, cells that have successfully edited display normal amounts of IgM due to the expression of nonautoreactive BCRs. Moreover, ~50% of the edited B cells in

3-83Igi,H-2<sup>b</sup> mice express Igλ L chain, likely because many newly expressed κ chains retain autoreactivity (Nemazee and Bürki, 1989; Braun et al., 2000). When we measured these parameters in CD24<sup>hi</sup> B cells from the bone marrow of P110\* autoreactive mice we found no detectable surface IgM or Igλ (Fig. 4 A). This was in striking contrast to their littermate controls in which ~10–15% of CD24<sup>hi</sup> B cells were IgM<sup>+</sup> and half of these expressed Igλ (Fig. 4 A). Although there was no detectable surface IgM, P110\* B cells had high levels of intracellular IgM (Fig. 4 B). Overall, these data indicate that P110\* autoreactive B cells retained expression of the autoreactive 3-83 BCR, which was likely internalized as a result of binding antigen.

Transcription of *RAG1* and *RAG2* genes is mediated by Forkhead box protein O1 (FOXO1), a protein negatively regulated by PI3K via AKT (Amin and Schlissel, 2008; Dengler et al., 2008). There was a significant twofold reduction in both FOXO1 protein (Fig. 4 C) and gene transcripts (Fig. 4 D, left) in bone marrow B cells of P110\* autoreactive mice relative to mb1Cre controls. P110\* cells also showed undetectable levels of *RAG1* and *RAG2* gene transcripts (Fig. 4 D, center and right). Another hallmark of edited B cells is a reduction of surface CD19 (Verkoczy et al., 2007; Duong et al., 2011; Lang et al., 2016), a coreceptor implicated in the activation of PI3K and in the positive selection of immature B cells (Diamant et al., 2005). CD19 was increased almost twofold, on average, on autoreactive immature B cells expressing P110\* (Fig. 4 E, top), although it was still below the level found on B cells from nonautoreactive 3-83Igi,H-2<sup>d</sup> mice (Fig. 4 E, bottom). Increased CD19 expression was also observed on P110\* nonautoreactive B cells, but the effect was more subtle than on autoreactive cells.

Upon surface expression of IgM, immature B cells upregulate B cell activating factor receptor (BAFFR), a receptor that promotes cell survival in response to the BAFF cytokine (Hsu et al., 2002; Gorelik et al., 2004; Rowland et al., 2010b). Expression of BAFFR, which is lower on autoreactive than nonautoreactive immature B cells (Rowland et al., 2010b), was 1.5-fold higher when autoreactive immature B cells expressed P110\*, although this was still below the expression observed on nonautoreactive cells (Fig. 4 F). Moreover, expression of BAFFR was increased by more than twofold on P110\* nonautoreactive B cells relative to their controls (Fig. 4 F), suggesting antigen-induced BCR signaling counteracts PI3K-mediated elevation of this receptor. In addition, the chemokine receptor C-X-C chemokine receptor type 4 (CXCR4), which is important for tissue retention of bone marrow B cells (Beck et al., 2014), was expressed approximately twofold less on both autoreactive and nonautoreactive immature B cells of P110\* mice relative to their respective controls (Fig. 4 F).

These data demonstrate that activation of PI3K prevents receptor editing in bone marrow autoreactive B cells and leads to changes in markers associated with cell survival and the selection of immature B cells into peripheral tissues.

### Activation of PI3K leads to the escape of high-avidity autoreactive B cells into peripheral lymphoid tissue

To test whether activation of PI3K is sufficient to bypass all mechanisms of central tolerance, including the survival and

bone marrow emigration of autoreactive B cells into the periphery, we compared the splenic B cell populations of P110\* mice and their littermate controls. Total B220<sup>+</sup> B cell numbers were reduced in the spleen of P110\* autoreactive (H-2<sup>b</sup>) mice relative to their littermate controls (Fig. 5 A). However, these numbers were similar to those of nonautoreactive mice with or without P110\*, and, more importantly, they were higher than in autoreactive 3-83Igi,H-2<sup>b</sup> *Rag1*<sup>-/-</sup> mice (Fig. 5 A) in which, due to a *RAG1* deficiency, autoreactive B cells cannot perform receptor editing and consequently succumb to clonal deletion in the bone marrow (Halverson et al., 2004; Liu et al., 2005).

We next examined if the spleen B cells of P110\* autoreactive mice had maintained their 3-83Ig autoreactive specificity. Similar to what observed in bone marrow, we could not initially detect B cells with surface Igλ or IgM in the spleen of 3-83Igi,H-2<sup>b</sup> P110\* mice (Fig. 5 B). This was also true for IgD (Fig. 5 C) and was in striking contrast to 3-83Igi,H-2<sup>b</sup> mb1Cre control mice in which, due to receptor editing, most B cells expressed IgM and ~50%, on average, expressed Igλ (Fig. 5 B). The absence of detectable IgM on the surface of P110\* autoreactive B cells was not caused by chronic activation of the PI3K pathway, because B cells from P110\* nonautoreactive 3-83Igi,H-2<sup>d</sup> mice had normal membrane expression of IgM (Fig. 5 D). We reasoned that the inability to detect IgM was caused by low retention of surface BCR, since the receptor was most likely internalized following autoantigen binding. To improve the detection of surface BCR, we incubated the cells with biotinylated anti-Ig antibodies and revealed these antibodies with fluorescent streptavidin. Indeed, using this method, we were able to detect on the surface of P110\* autoreactive B cells low amounts of 3-83Ig H+κ, 3-83κ, and IgM that were clearly above the fluorescence detected on negative control (B220<sup>-</sup>) cells but ~10-fold below what we measured on nonautoreactive 3-83Ig<sup>+</sup> cells (Fig. 5 E). Because intracellular staining of 3-83Ig is not feasible (Liu et al., 2005), we confirmed the presence of internalized antigen receptor by measuring the expression of intracellular IgM, which was within the same range in P110\* and control autoreactive B cells (Fig. 5 F).

Lupus-prone MRL/*lpr* mice exhibit gross deficiencies in central B cell tolerance, with defects in receptor editing (Lamoureux et al., 2007) and accumulation of autoreactive B cells in the periphery (Fournier et al., 2012). Thus, we asked whether this phenotype is associated with higher activity of the PI3K pathway during B cell development. Indeed, higher amounts of pAKT-S473, but not pAKT-T308, were observed in bone marrow developing B cells of MRL/*lpr* mice relative to CB17 healthy mice (Fig. S2 C).

Overall, these data demonstrate that constitutive activation of PI3K allows high-avidity autoreactive B cells to circumvent mechanisms of central tolerance by forgoing receptor editing and clonal deletion and escaping from the bone marrow to establish peripheral residence.

### Activation of PI3K leads to altered differentiation and organization of splenic autoreactive and nonautoreactive B cells

Once autoreactive immature B cells escape from the bone marrow, they undergo serial checkpoints of peripheral tolerance



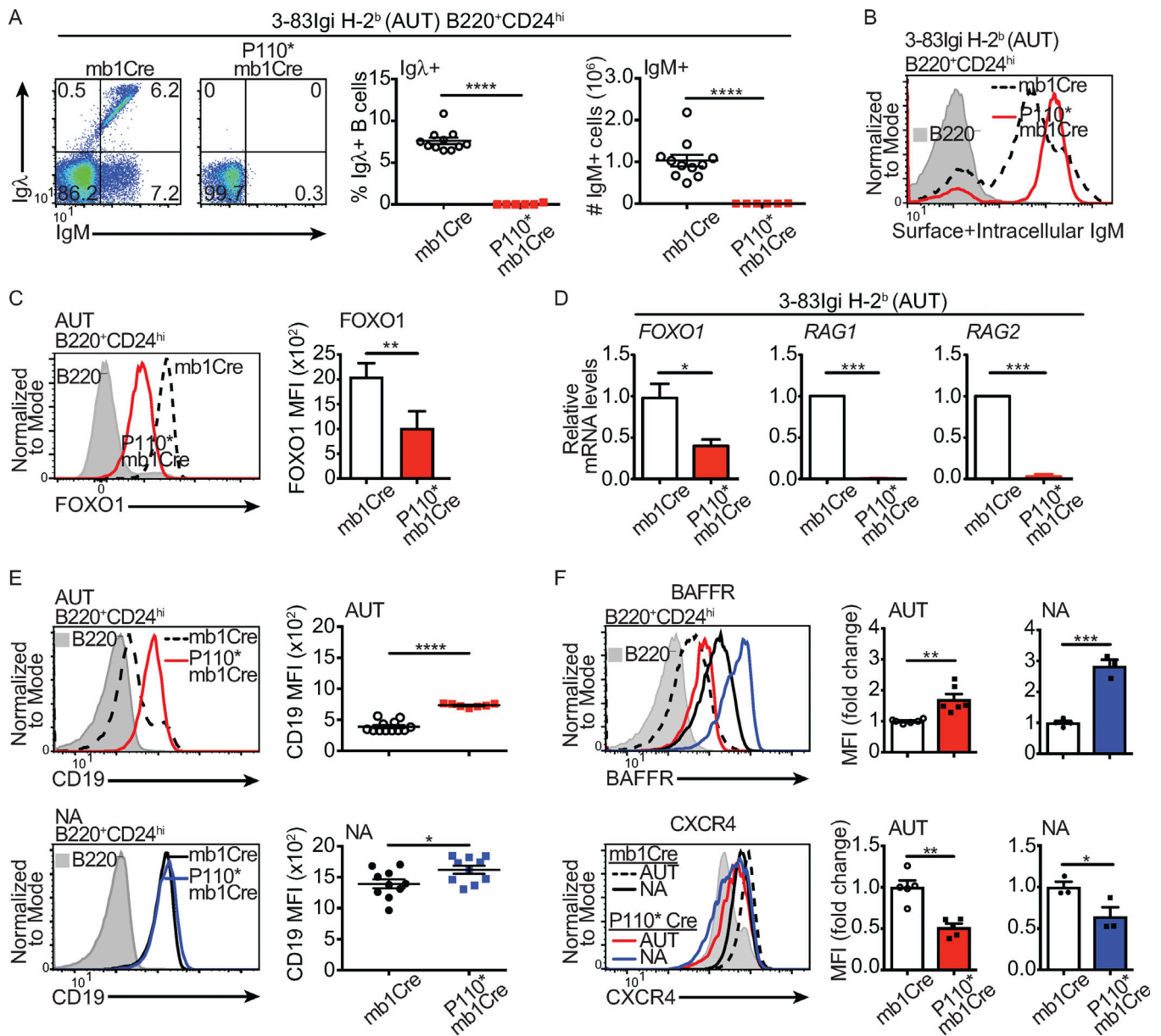


**Figure 4. Activation of PI3K abrogates receptor editing in high-avidity autoreactive immature B cells.** (A) Representative analysis (flow plots) and quantification (graphs) of immature (B220<sup>+</sup>CD24<sup>hi</sup>) B cells expressing Igλ (shown as frequency) or IgM (shown as absolute cell numbers) in the bone marrow of autoreactive (AUT) 3-83Igi,H-2<sup>b</sup> mb1Cre (*n* = 11) and P110<sup>\*</sup>-mb1Cre (*n* = 6) mice analyzed in at least four independent experiments. (B) Representative flow cytometric analysis (of three experiments) of total (surface and intracellular) IgM in bone marrow B220<sup>+</sup>CD24<sup>hi</sup> immature B cells of mb1Cre (black dashed line) and P110<sup>\*</sup>-mb1Cre (red intact line) autoreactive (AUT) mice. The gray shaded histogram represents B220<sup>-</sup> cells, which are negative for IgM. (C) Flow cytometric quantification of FOXO1 protein in B220<sup>+</sup>CD24<sup>hi</sup> immature B cells from indicated mice. *n* = 3 in each group from one out of two experiments. (D) Relative *Foxo1*, *Rag1*, and *Rag2* mRNA levels in B220<sup>+</sup> or B220<sup>+</sup>GFP<sup>+</sup> cells sorted from the bone marrow of autoreactive mb1Cre or P110<sup>\*</sup>-mb1Cre mice, respectively. Data were normalized to 18S mRNA levels and are expressed as fold change over the average mRNA levels in 3-83Igi,H-2<sup>b</sup> mb1Cre cells. *n* = 3 mice in each group from one experiment. FOXO1 protein in C and *Foxo1* RNA in D were analyzed in independent experiments. (E) Representative flow cytometric analysis and overall quantification of CD19 expression on immature (B220<sup>+</sup>CD24<sup>hi</sup>) B cells from autoreactive (top) and nonautoreactive (NA; bottom) mice, either mb1Cre (*n* = 12 and 10, respectively) or P110<sup>\*</sup>-mb1Cre (*n* = 7 and 10, respectively), from five independent experiments. (F) Flow cytometric analyses and quantification of the expression of BAFFR (top) and CXCR4 (bottom) on bone marrow immature (B220<sup>+</sup>CD24<sup>hi</sup>) B cells from autoreactive and nonautoreactive mb1Cre and P110<sup>\*</sup>-mb1Cre mice (*n* = 3–6 per group from at least two independent experiments). In all flow analyses, GFP gating was additionally applied to cells from P110<sup>\*</sup>-mb1Cre mice. Data shown in all panels represent the mean ± SEM. P values were calculated using a one-tailed Mann-Whitney *U* test in A, E, and F and a one-tailed unpaired *t* test in C and D. \*, *P* ≤ 0.05; \*\*, *P* ≤ 0.01; \*\*\*, *P* ≤ 0.001; \*\*\*\*, *P* ≤ 0.0001.

aimed to prevent their participation in immune responses (Goodnow et al., 2010). The first of these is a checkpoint between the transitional and mature B cell stages. To determine whether activation of PI3K breaks the early stages of peripheral

tolerance, we used flow cytometry to examine the expression of markers indicative of transitional (T), follicular (FO), and marginal zone (MZ) B cell subsets within the spleen of P110<sup>\*</sup> and control mice (Fig. 6, A and B; and Fig. S3). There was a virtual

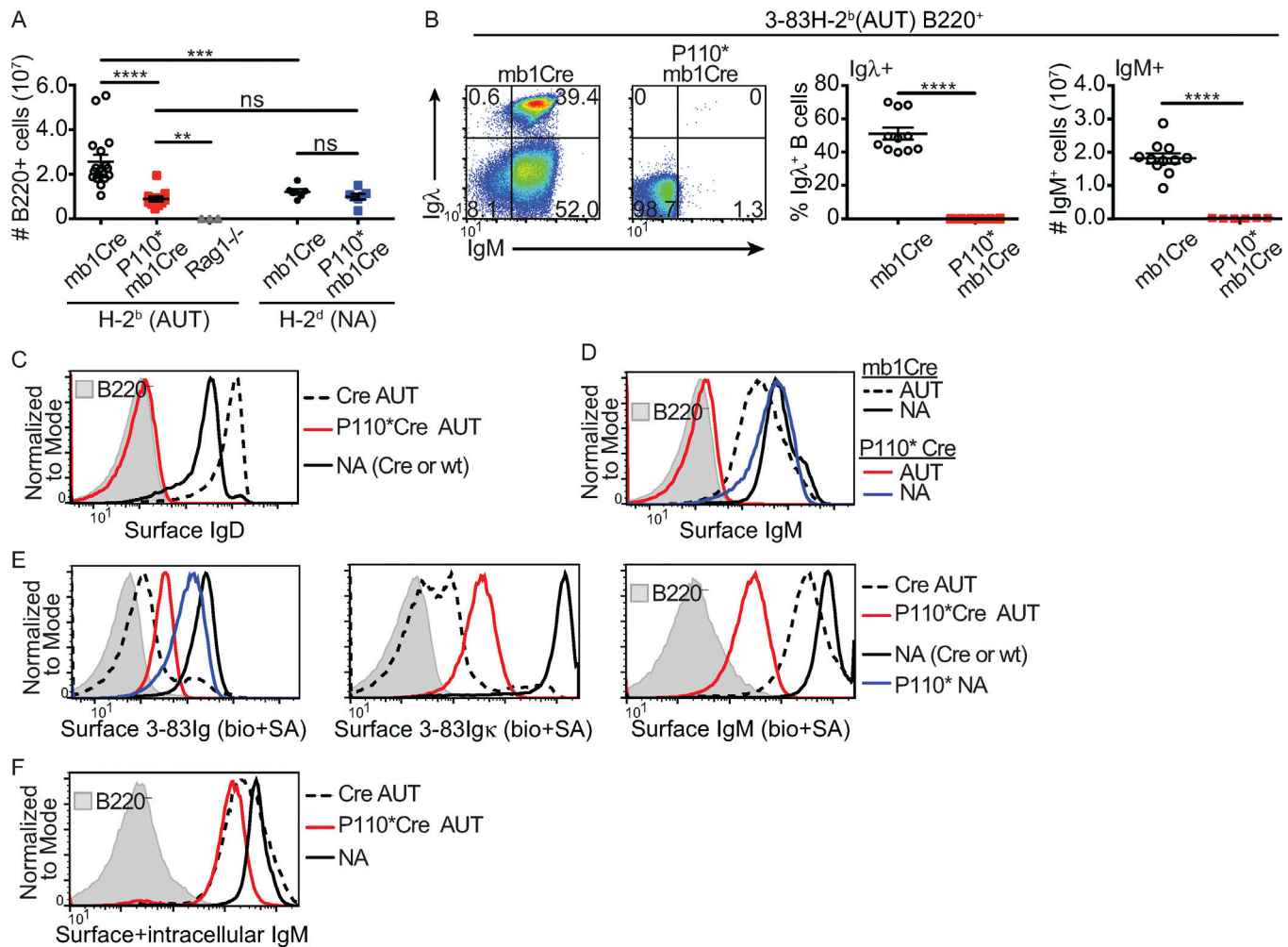


**Figure 5. Activation of PI3K promotes export of high-avidity autoreactive B cells into peripheral lymphoid tissue. (A)** Absolute numbers of B220<sup>+</sup> cells in the spleen of autoreactive (AUT) 3-83Igi,H-2<sup>b</sup> mice with mb1Cre (*n* = 17), P110\*<sup>-</sup>mb1Cre (*n* = 12), or Rag1<sup>-/-</sup> (*n* = 3) analyzed in a total of seven experiments and nonautoreactive (NA) 3-83Igi,H-2<sup>d</sup> mice with mb1Cre (*n* = 6) or P110\*<sup>-</sup>mb1Cre (*n* = 7) analyzed in three experiments. **(B)** Representative flow analysis and quantification of B220<sup>+</sup> B cells expressing Igλ (shown as frequency) and IgM (shown as absolute cell numbers) in the spleen of autoreactive mb1Cre (*n* = 11) and P110\*<sup>-</sup>mb1Cre (*n* = 6) mice analyzed in four independent experiments. Data in A and B show the mean ± SEM. **(C and D)** Representative analyses (of at least six mice per strain and three experiments) of surface IgD (C) and IgM (D) measured with fluorochrome-conjugated antibodies on splenic B220<sup>+</sup> B cells from the indicated mice. B220<sup>-</sup> cells are shown as negative control. **(E)** Flow cytometric analyses (representative of at least three mice per strain and two experiments) of surface 3-83Ig H+κ, 3-83Igκ, and IgM on B220<sup>+</sup> B cells from the spleen of autoreactive mb1Cre and P110\*<sup>-</sup>mb1Cre mice and nonautoreactive mice. These analyses were performed by staining with biotin-conjugated antibodies followed by PE-conjugated streptavidin (SA) to amplify the signal. The gray shaded histograms represent B220<sup>-</sup> cells as a negative control. **(F)** Representative analysis (one of three experiments) of total (surface and intracellular) IgM expression in B220<sup>+</sup> cells from the spleen of indicated mice. The gray shaded histogram represents B220<sup>-</sup> negative control cells. In all flow analyses, GFP gating was additionally applied to cells from P110\*<sup>-</sup>mb1Cre mice. P values were calculated using a one-tailed Mann-Whitney *U* test. \*\*, *P* ≤ 0.01; \*\*\*, *P* ≤ 0.001; \*\*\*\*, *P* ≤ 0.0001; ns, not significant.

absence of MZ B cells, which are characterized by high expression of CD21 and CD1d, in the spleen of P110\* autoreactive (H-2<sup>b</sup>) mice (Fig. 6 A). This was surprising given that mb1Cre control autoreactive mice displayed a large MZ B cell subset, larger than in nonautoreactive mice. Moreover, a sizable body of literature indicates that PI3K activity in B cells positively correlates with MZ B cell formation (Anzelon et al., 2003; Durand et al., 2009; Chen et al., 2010; Kövesdi et al., 2010; So et al., 2013). In fact, the splenic B cell population of nonautoreactive (H-2<sup>d</sup>) P110\* mice was enriched in MZ B cells (Fig. 6 B). The absence of MZ B cells in P110\* autoreactive mice was accompanied by a significant decrease in the CD24<sup>hi</sup>CD23<sup>hi</sup>CD21<sup>hi</sup> transitional T2

population (Fig. 6 A), which comprises MZ B cell precursors (Srivastava et al., 2005). Transitional T1 cells, in contrast, were present (and modestly increased) in both autoreactive and nonautoreactive P110\* mice (Fig. 6, A and B).

Although P110\* autoreactive B cells did not differentiate into T2 and MZ B cells, most displayed decreased expression of CD24 and CD93 (Fig. 6, A and C), a phenotype compatible with mature B cells. Moreover, a fraction of these cells expressed CD23 (Fig. 6, A and C), a marker of mature FO B cells. The expression of CD23, however, was generally reduced on CD24<sup>low</sup>CD1d<sup>low</sup>CD21<sup>low</sup> non-MZ mature B cells of both autoreactive and nonautoreactive P110\* mice (Fig. 6 D), an observation consistent with that of



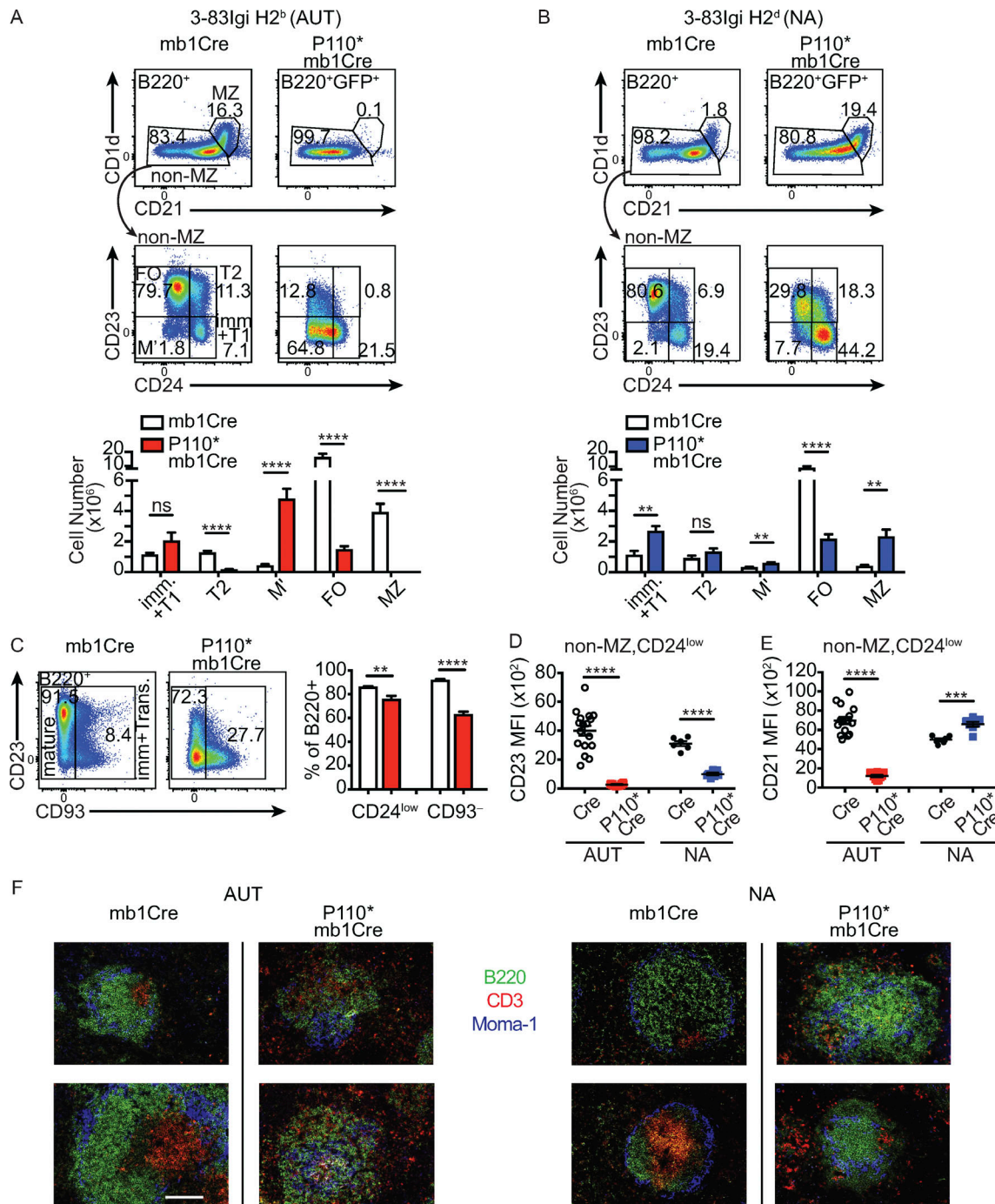


**Figure 6. PI3K activation leads to the maturation of autoreactive B cells and to the formation of disorganized follicles. (A and B)** Gating strategy and bar graph quantification of B cell subsets in the spleen of autoreactive (AUT) mice (A;  $n = 15$  mb1Cre and 10 P110\*, six experiments) and nonautoreactive (NA) mice (B;  $n = 6$  mb1Cre and 7 P110\*, three experiments). B220<sup>+</sup> and B220<sup>+</sup>GFP<sup>+</sup> cells were gated as shown in Fig. S3. B cell subsets were discriminated as MZ B cells (B220<sup>+</sup>CD1d<sup>hi</sup>CD21<sup>hi</sup>), immature and transitional T1 B cells (B220<sup>+</sup>CD1d<sup>low</sup>CD24<sup>hi</sup>CD23<sup>-</sup>), transitional T2 B cells (B220<sup>+</sup>CD1d<sup>low</sup>CD24<sup>hi</sup>CD23<sup>+</sup>), FO B cells (B220<sup>+</sup>CD1d<sup>low</sup>CD24<sup>low</sup>CD23<sup>+</sup>), and M' B cells (B220<sup>+</sup>CD1d<sup>low</sup>CD24<sup>low</sup>CD23<sup>low</sup>). **(C)** Top: Representative flow cytometric analysis showing CD93 expression on spleen B220<sup>+</sup> (or B220<sup>+</sup>GFP<sup>+</sup>) B cells from autoreactive mb1Cre and P110\*-mb1Cre mice, respectively. Bottom: Mean percentages of CD24<sup>low</sup> (shown in A) and CD93<sup>-</sup> mature B cells within B220<sup>+</sup> (or B220<sup>+</sup>GFP<sup>+</sup>) B cells in the spleen of autoreactive mb1Cre (white bars) and P110\*-mb1Cre (red bars) mice.  $n = 8$ –10 mice per group in at least four experiments. **(D and E)** Quantification of CD23 (D) and CD21 (E) surface expression (MFI) on splenic B220<sup>+</sup>CD1d<sup>low</sup>CD24<sup>low</sup> mature B cells (gated as in A and B) from individual autoreactive mice ( $n = 15$  mb1Cre and 10 P110\*, seven experiments) and nonautoreactive mice ( $n = 6$  mb1Cre and 7 P110\*, three experiments). **(F)** Representative immunofluorescence staining at 100 $\times$  magnification of B220 (green), CD3 (red), and Moma-1 (blue) in tissue sections obtained from the spleen of indicated autoreactive (left) and nonautoreactive (right) mice. Two representative images are shown for each strain. The white bar in the bottom left equals 500  $\mu$ m. Data are representative of two spleens from each strain analyzed during two independent experiments. In all flow analyses, GFP gating was additionally applied to cells from P110\*-mb1Cre mice. Data shown in A–D represent the mean  $\pm$  SEM. P values were calculated using a one-tailed Mann-Whitney  $U$  test in A and B and a one-tailed unpaired  $t$  test in C–E. \*\*,  $P \leq 0.01$ ; \*\*\*,  $P \leq 0.001$ ; \*\*\*\*,  $P \leq 0.0001$ ; ns, not significant.

other mice with higher PI3K activity in B cells (Srinivasan et al., 2009; Getahun et al., 2016). In contrast, the expression of CD21, which was increased in bone marrow B cells of P110\* mice (Figs. 3 C and S1 E), was higher only on (non-MZ) mature B cells of nonautoreactive P110\* mice compared with their controls (Fig. 6 E). P110\* autoreactive B cells displayed a dramatic reduction of CD21 (Fig. 6 E), a phenotype that was therefore dependent on autoreactivity. Due to the phenotypic changes caused by the expression of P110\*, we subdivided the splenic B cells into conventional T1 (CD24<sup>hi</sup>CD23<sup>low</sup>), T2 (CD24<sup>hi</sup>CD23<sup>hi</sup>), FO (CD24<sup>low</sup>CD23<sup>hi</sup>), and MZ (CD21<sup>hi</sup>CD1d<sup>hi</sup>) B cell subsets and added an M' (CD24<sup>low</sup>CD23<sup>low</sup>) mature cell population (Fig. 6, A and B). Quantification of these subsets clearly shows that while P110\* nonautoreactive mature B cells equally distribute into FO and MZ B populations, P110\* autoreactive mature cells are mostly M' (Fig. 6, A and B).

Given the changes imparted by P110\* and self-reactivity on the expression of markers used for the definition of FO B cells, we next used immunofluorescent histology to evaluate the ability of B cells to form follicles. Tissue sections were stained for B220, CD3, and MOMA-1 to distinguish B cell, T cell, and MZ cell areas, respectively (Fig. 6 F). B cells of P110\* mice were found in follicles, but the structure of these follicles was greatly disorganized, particularly in the autoreactive mice. Specifically, the FO B cells of P110\* H-2<sup>b</sup> mice were not confined within a MZ sinus delineated by MOMA-1-expressing macrophages that surround follicles and as observed in the spleen of littermate controls (Fig. 6 F). Moreover, T cells, which are usually organized in areas adjacent to the B cell follicles (Fig. 6 F, mb1Cre), were dispersed throughout the follicle and within the red pulp in the spleen of autoreactive P110\* mice (Fig. 6 F, left). This phenotype was also observed in nonautoreactive P110\* animals, but to a lesser extent (Fig. 6 F, right). When the follicles in sections were screened blindly, 100% of the follicles in the spleen of autoreactive P110\* mice were considered disorganized, while this frequency was ~40% for nonautoreactive P110\* mice.

Taken together, these data show that activation of PI3K allows high-avidity autoreactive B cells to reach a mature stage in the spleen and thus bypass not only mechanisms of central tolerance but also initial checkpoints of peripheral tolerance. However, chronic activation of PI3K leads to changes in B cells that affect the organization of follicles and the tissue localization of T cells, with more severe changes in mice in which the B cells are autoreactive.

#### High-avidity autoreactive B cells that express P110\* undergo activation in response to self-antigen and produce autoantibodies in vitro, but not in vivo

Markers of activation and plasmablast differentiation were analyzed to establish whether P110\* autoreactive B cells display signs of productive antigen encounter. We found a dramatic increase (5- to 10-fold) in the frequency of B cells expressing CD69, CD86, and CD138 in the spleen of autoreactive P110\* mice relative to their controls (Fig. 7, A-C). Furthermore, CD69 mean fluorescence intensity (MFI) was more than doubled in the CD23<sup>+</sup> fraction of autoreactive P110\* B cells (Fig. 7 D), a change reflecting a higher frequency of CD69<sup>+</sup> cells (Fig. 7 D, histogram)

and not observed for CD86. With the exception of a small increase in CD86<sup>+</sup> cells (Fig. 7 B), these changes were not detected in nonautoreactive P110\* B cells (Fig. 7, A-D), and thus, they most likely reflect P110\* autoreactive B cells undergoing activation in response to binding the cognate H-2K<sup>b</sup> self-antigen.

Deficiency in the PI3K negative regulators PTEN and SHIP-1 break anergy in low-avidity autoreactive B cells, leading to increased cell activation as well as the development of autoantibody-secreting cells (Getahun et al., 2016). However, despite the presence of activated B cells and of cells with a CD138<sup>+</sup> plasmablast phenotype, neither 3-83IgM nor 3-83IgG autoantibodies were detected in sera of autoreactive P110\* mice (Fig. 8, A and B). In contrast, these antibodies were readily measured in the sera of nonautoreactive P110\* mice, with 3-83IgM reaching higher concentrations relative to littermate controls (Fig. 8 A). Low amounts of total IgM and IgG were measured in the sera of autoreactive P110\* mice (Fig. S4 A). These Igs were likely the product of B cells that failed to express P110\* and had edited their specificity, a conclusion implied by the presence of a small number of GFP<sup>-</sup> B cells (<10% of all B cells), some of which expressed Igλ (Fig. S4, B and C) and secreted Igλ (Fig. S4 D).

We reasoned that the absence of secreted 3-83Igs in autoreactive P110\* mice was due to T cell tolerance and the lack of cognate T cells reacting with K<sup>b</sup> peptides. Indeed, autoreactive P110\* B cells were able to secrete 3-83IgM and 3-83IgG upon culture with the surrogate T cell help factors anti-CD40 antibodies and IL-4 (Fig. 8 C). In addition, we found that P110\* mice had a significant reduction of the T FO helper (T<sub>FH</sub>) splenic cell population, defined as CD3<sup>+</sup>CD4<sup>+</sup>PD-1<sup>+</sup>CXCR5<sup>+</sup> (Fig. S5, A-C). Together, these observations suggested the possibility that the absence of secreted 3-83Igs in autoreactive P110\* mice was caused by a lack of T cell help.

To determine if the provision of T cell help to autoreactive P110\* B cells in vivo was able to stimulate the production of 3-83 autoantibodies in P110\* autoreactive mice, we had to resort to methods that did not involve BCR stimulation. This was because of the extremely low amounts of Ig antigen receptor present on the surface of P110\* autoreactive B cells. We also had to use methods that elicited cognate help from T cells reactive with an antigen other than K<sup>b</sup> because of the absence of T cells reactive with K<sup>b</sup> peptides in H-2<sup>b</sup> mice. In published studies, antigens targeted to CD19 via anti-CD19 mAbs were internalized and processed by B cells (Yan et al., 2005) and then presented to CD4 T cells inducing their activation (Yan et al., 2005; Ma et al., 2013). Thus, we used this system to target the protein antigen PE to CD19 expressed by B cells in P110\* autoreactive mice (as shown in Fig. S5 D), cells that were confirmed to express MHC-II (Fig. S5 E). Mice were first immunized with PE in Alum to prime PE-reactive T cells and then injected with PE-conjugated anti-CD19 mAbs 1 wk later. 2 wk after this treatment, however, we were unable to detect 3-83 antibodies in sera of autoreactive P110\* mice (Fig. 8 D). This approach failed also to raise total serum Ig levels in either P110\* or control mice (Fig. 8 E). As an alternative system by which to deliver T cell help, we chose to transfer T cells from mice expressing the MHC-II mutant allele I-A<sup>bm12</sup> (bm12 mice), which differs from I-A<sup>b</sup> by three amino

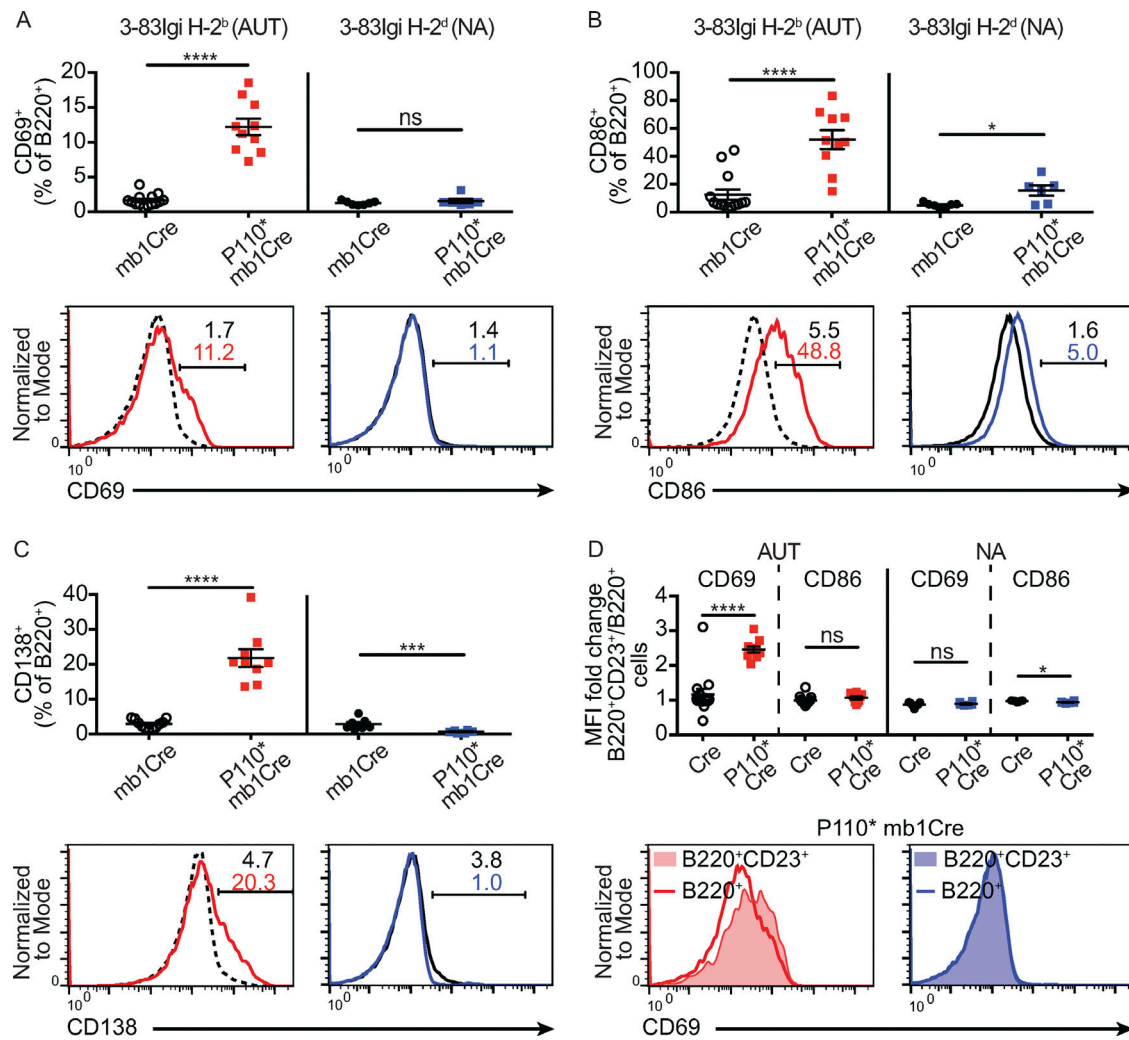


**Figure 7. Activation and plasmablast differentiation of P110\* autoreactive B cells in response to self-antigen. (A–C)** Frequencies and representative analyses of B220<sup>+</sup> (or B220<sup>+</sup>GFP<sup>+</sup>) B cells expressing CD69 (A), CD86 (B), or CD138 (C) in the spleen of autoreactive (AUT) mb1Cre (open circles and black dashed lines, *n* = 11–14) or P110\*–mb1Cre (close red squares and red intact lines, *n* = 9–10) mice and nonautoreactive (NA) mb1Cre (closed black circles and black intact lines, *n* = 7) or P110\*–mb1Cre (close blue squares and blue intact lines, *n* = 6) mice. Data are from three or more experiments for each group of mice. **(D)** Top: Change in the expression of CD69 and CD86 (MFI fold change) on B220<sup>+</sup>CD23<sup>+</sup> spleen B cells relative to total B220<sup>+</sup> cells in individual autoreactive and nonautoreactive mb1Cre and P110\*–mb1Cre mice. Bottom: Representative analyses of CD69 on B220<sup>+</sup> and B220<sup>+</sup>CD23<sup>+</sup> cells in P110\* autoreactive (left) and nonautoreactive (right) mice. Number of mice per group and experiments are as listed for A–C. Data in all panels show the mean ± SEM. P values were calculated using a one-tailed Mann–Whitney *U* test. \*, *P* ≤ 0.05; \*\*\*, *P* ≤ 0.001; \*\*\*\*, *P* ≤ 0.0001; ns, not significant.

acids. This mutation evokes bm12 CD4 T cells to recognize and activate any B cell expressing I-A<sup>b</sup>, as evidenced by the production of anti-DNA autoantibodies in I-A<sup>b</sup> wild-type mice adoptively transferred with bm12 spleen cells (Morris et al., 1990; Eisenberg and Via, 2012). Thus, B cell-depleted bm12 splenic cells were injected into autoreactive P110\* and control mice and 3–83Ig measured in sera 2 wk later. As with the previous method, however, we did not observe any increase of 3–83 autoantibodies in the serum of mice that had received bm12 cells (Fig. 8 D). This treatment was also unable to raise total Ig levels (Fig. 8 E), although it did increase (by almost 10-fold) serum levels of anti-DNA antibodies in wild-type mice (Fig. S5 F).

Taken together, these data indicate that in vivo, T cell help is unable to elicit antibody production by high-avidity autoreactive B cells that express P110\*.

## Discussion

Central B cell tolerance is crucial to the development of a circulating B cell repertoire devoid of high-avidity autoreactive specificities, but the molecular checkpoints that enforce this process are still poorly understood. Our findings demonstrate that activation of the PI3K pathway in high-avidity autoreactive immature B cells, to levels comparable of those in nonautoreactive cells, completely abrogates receptor editing, prevents clonal deletion, and supports ongoing differentiation and migration of the autoreactive cells into the peripheral tissue. Once in the periphery, active PI3K enables high-avidity autoreactive B cells to undergo differentiation into FO B cells and activation in response to self-antigen, but not to secrete autoantibodies.

Once immature B cells express Ig H and L chains that form nonautoreactive BCRs, these unbound membrane BCRs transduce



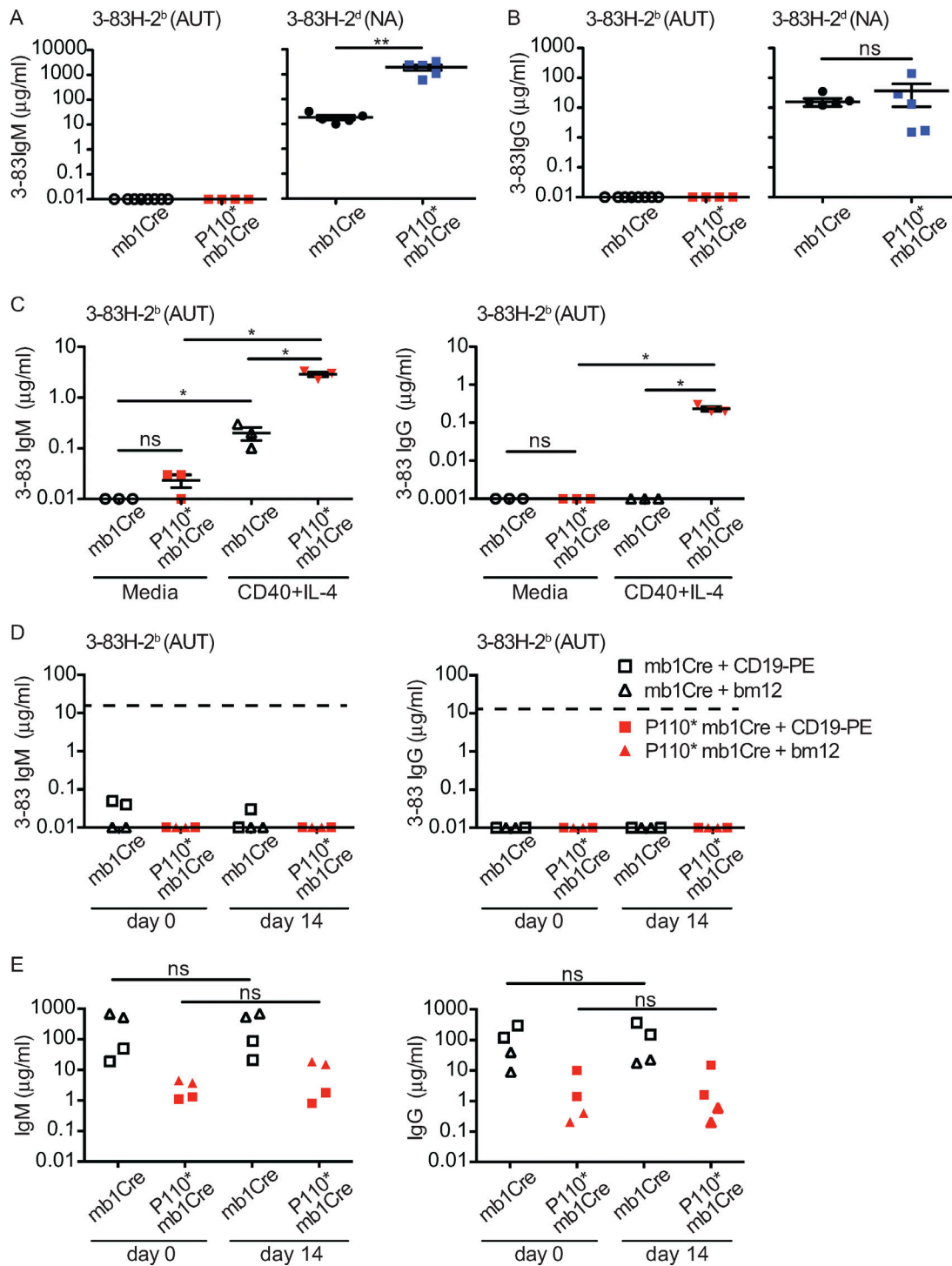


**Figure 8. Activation of PI3K causes production of high-avidity autoantibodies in response to T cell help in vitro, but not in vivo. (A and B)** Concentration ( $\mu\text{g/ml}$ ) of 3-83IgM (A) and 3-83IgG (B) in sera of mb1Cre and P110<sup>\*</sup>-mb1Cre mice on either the autoreactive (AUT) 3-83Igi,H-2<sup>b</sup> ( $n = 8$  and 4) or the nonautoreactive (NA) 3-83Igi,H-2<sup>d</sup> ( $n = 5$ ) backgrounds analyzed in two experiments. **(C)** Concentration ( $\mu\text{g/ml}$ ) of 3-83IgM and 3-83IgG in the supernatant of splenic B cells from autoreactive mb1Cre and P110<sup>\*</sup>-mb1Cre mice cultured for 8 d in either media alone or in the presence of anti-CD40 antibodies and IL-4.  $n = 3$  per group from two independent experiments. **(D and E)** Concentration ( $\mu\text{g/ml}$ ) of 3-83IgM and 3-83IgG (D) and total IgM and IgG (E) in the sera of autoreactive mb1Cre or P110<sup>\*</sup>-mb1Cre mice before (day 0) and on day 14 after the injection of either anti-CD19-PE antibodies or the transfer of bm12 (B220<sup>-</sup>) spleen cells.  $n = 2$  for each experimental condition, representative of two independent experiments. The dashed lines in D indicate the reference levels of 3-83IgM and 3-83IgG in 3-83Igi,H-2<sup>d</sup> mice. Data in A–C show the mean  $\pm$  SEM. Data were analyzed using a one-tailed Mann–Whitney *U* test. \*,  $P \leq 0.05$ ; \*\*,  $P \leq 0.01$ ; ns, not significant.

tonic signals that trigger a developmental pathway that halts Ig gene recombination and promotes the generation of functional mature B cells (Monroe, 2006; Pelanda and Torres, 2012). In past studies, we have shown that nonautoreactive immature B cells, via their tonic BCR signaling, activate ERK to twice the levels observed in high-avidity autoreactive cells (Teodorovic et al., 2014). However, activating ERK in 3-83Ig<sup>+</sup> autoreactive B cells by the expression of a constitutively active form of MEK1 did not break central tolerance (Greaves et al., 2018). We now show that the PI3K pathway (measured by phosphorylation of AKT-T308) is also twice as active in 3-83Ig<sup>+</sup> nonautoreactive compared with autoreactive cells, an observation that is in agreement with past studies of PIP3 quantification in immature B cells treated or not with anti-BCR antibodies in culture (Verkoczy et al., 2007). Our new findings, when integrated with previous observations from PI3K gene deletion studies (Llorian et al., 2007; Verkoczy et al., 2007), indicate that the low amount of PI3K activity observed in high-avidity autoreactive immature B cells is required for ongoing Ig gene recombination (i.e., receptor editing), while the higher PI3K activity present in nonautoreactive immature B cells is required to terminate Ig gene recombination and promote differentiation. Thus, the PI3K pathway controls both negative and positive selection of immature B cells, at least in mice. Whether this is also true for developing human B cells remains to be investigated, but the possibility is supported by the fact that one third of individuals bearing gain-of-function mutations in PI3K exhibit autoantibodies and other autoimmune manifestations (Coulter et al., 2017), a finding that was recapitulated in mice with similar mutations (Preite et al., 2018). Furthermore, increased PI3K activity has been recorded in peripheral B cells of mice with lupus-like disease and of lupus patients, when compared with B cells of healthy individuals (Wu et al., 2007; Suárez-Fueyo et al., 2011). We show here that bone marrow developing B cells from MRL/lpr lupus mice have slightly but significantly higher phosphorylation of AKT at S473 (though not at T308) relative to cells of healthy mice. Thus, it is tempting to speculate that dysregulated activation of PI3K contributes to the central tolerance defects that have been described in B cells of lupus mice (Lamoureux et al., 2007; Fournier et al., 2012) and patients (Meffre, 2011).

The basal activation of the PI3K pathway in immature B cells is likely regulated by a combination of tonic BCR and CD19 signaling (Otero et al., 2001; Verkoczy et al., 2005; Llorian et al., 2007; Aiba et al., 2008), which are both present in nonautoreactive immature B cells and significantly diminished in high-avidity autoreactive cells (Verkoczy et al., 2007; Teodorovic et al., 2014). When PI3K was activated in IgM<sup>-</sup> bone marrow pre-B cell cultures, it led to the AKT-mediated phosphorylation and degradation of FOXO1, halting the expression of the RAG genes (Amin and Schlissel, 2008). Our data demonstrate that even in high-avidity autoreactive IgM<sup>+</sup> B cells and in vivo, activation of PI3K to physiologically relevant levels leads to reduced amounts of FOXO1, loss of RAG expression, and the termination of receptor editing. PI3K activation also increased the expression of both CD19 and BAFFR. Although the abundance of these membrane proteins on P110\* autoreactive cells did not reach that observed on

nonautoreactive B cells, based on previous studies (Otero et al., 2003; Otero and Rickert, 2003; Sasaki et al., 2004; Rowland et al., 2010b), we speculate that their increased expression contributed to the ongoing survival and maturation of autoreactive B cells. Importantly, expression of P110\* also led to increased levels of pERK in autoreactive cells, which was probably achieved via regulating the RAS pathway (Ramadani et al., 2010; Okkenhaug, 2013). Although increased ERK activation by itself is unable to break tolerance (Greaves et al., 2018), we cannot exclude that some of the changes observed in P110\* autoreactive B cells were indirectly mediated by PI3K via the RAS-ERK pathway.

Studies in mouse models of tolerance have demonstrated that when receptor editing is prevented, immature autoreactive B cells undergo clonal deletion (Chen et al., 1995; Halverson et al., 2004). Our findings extend previous in vitro studies (Browne et al., 2009; Cheng et al., 2009) to indicate that enhanced activation of the PI3K pathway protects autoreactive B cells from clonal deletion in vivo. This is demonstrated by the finding that, despite the abrogation of receptor editing, the numbers of B cells in the bone marrow and spleen of autoreactive P110\* mice were similar or even higher than those in nonautoreactive P110\* mice. Nevertheless, we note that the overall bone marrow B cell numbers were decreased (three- to fivefold) in P110\* relative to control mice. This phenotype was unrelated to the presence of the self-antigen and was due to a specific reduction of CD24<sup>hi</sup>CD2<sup>+</sup>CD21<sup>-</sup>CD23<sup>-</sup> pre-B/immature B cell numbers, a finding in agreement with older observations in mice bearing B cells that lack SHIP (Liu et al., 1998; Leung et al., 2013) and with recent observations in mice and patients expressing the active PI3K form PI3KCD-E1020K (Dulau Florea et al., 2017; Avery et al., 2018; Wray-Dutra et al., 2018). In PI3KCD-E1021K mice, the diminished numbers of pre-B/immature B cells was ascribed to reduced B cell survival (Wray-Dutra et al., 2018). Our finding of reduced IL-7R expression on P110\* bone marrow B cells, together with the known function this receptor plays in early B cell survival (Corfe and Paige, 2012), suggests this likely contributes to the cell survival defect observed in mice with enhanced PI3K activity.

Within the bone marrow tissue of P110\* autoreactive mice, a significant fraction of high-avidity autoreactive immature B cells up-regulated CD21, a marker of transitional B cells. These cells were also able to exit the bone marrow and home to the peripheral lymphoid tissue. We suggest this was likely achieved by reducing the expression of the chemokine receptor CXCR4, a receptor that is crucial for the retention of B cells in bone marrow tissue (Beck et al., 2014) and is expressed at higher levels on autoreactive than nonautoreactive immature B cells (Fig. 4 F). In the spleen, these high-avidity autoreactive B cells were able to differentiate further into mature B cells, thus indicating that higher activity of the PI3K pathway can also break initial checkpoints of peripheral B cell tolerance. This was in spite of the fact that the autoreactive P110\* B cells retained only one tenth or less of the BCR on the cell surface relative to edited and nonautoreactive B cells. The splenic B cell population of P110\* mice, however, exhibited a reduced proportion of mature B cells. This phenotype is reminiscent of that in patients and mice with PI3K gain-of-function mutations (Avery et al., 2018; Preite

et al., 2018; Wray-Dutra et al., 2018). Moreover, mature B cells of P110\* autoreactive mice had an unusual phenotype, which we labeled M'. CD23 expression was markedly diminished (by ~10-fold) by the expression of P110\*, a finding in line with previous reports of mice with enhanced PI3K activity (Srinivasan et al., 2009; Getahun et al., 2016) or deletion of FOXO1 (Dengler et al., 2008; Chen et al., 2010) in B cells. Interestingly, the expression of CD21 was also greatly decreased (by approximately sixfold) on P110\* splenic B cells, but only in autoreactive mice. This suggests that the reduced CD21 expression on P110\* autoreactive B cells was the consequence of chronic self-antigen encounter, a phenomenon well described in chronic human infections (Portugal et al., 2017). Despite abnormal CD21 and CD23 expression, we conclude that most of the autoreactive splenic P110\* B cells, including the M', were FO B cells. This was based on the down-regulation of both CD24 and CD93, which are markers for transitional B cells, the low expression of CD1d, a marker of MZ B cells, and the up-regulation (although blunted) of both CD21 and CD23, which are markers for FO B cells. Moreover, by using fluorescence microscopy, we were able to visualize B cell follicles in the spleen of both autoreactive and nonautoreactive P110\* mice.

A striking finding was the complete absence of MZ B cells in autoreactive P110\* mice. Increased activation of the PI3K pathway leads to augmented MZ B cell production (Anzelon et al., 2003; Suzuki et al., 2003; Chen et al., 2010; Avery et al., 2018; Preite et al., 2018; Wray-Dutra et al., 2018), and indeed, this was observed in nonautoreactive P110\* mice. Furthermore, some mouse strains with peripheral autoreactive B cells that bind self-antigen with low avidity display larger MZ B cell subsets (Li et al., 2002; Wen et al., 2005). This leads us to conclude that high-avidity autoreactive B cells, even when recruited into the spleen and provided constitutively active PI3K, are excluded from entering the MZ cell subset, and this is likely due to high levels of BCR signaling (Cariappa et al., 2001). The follicles in the spleen of P110\* mice, and particularly those in autoreactive animals, were partly disorganized. The B cells formed B cell areas, suggesting proper response to relevant chemokines and integrins. However, T cells were dispersed among B cells and in the red pulp. This abnormal T cell localization was associated with a virtual absence of T<sub>FH</sub> cells (Fig. S5, B and C). These surprising observations indicate that abnormal function of PI3K in B cells has a profound, indirect impact on the tissue localization and function of T cells.

B cells of P110\* autoreactive mice showed signs of activation in response to self-antigen, with 10–80% of spleen B cells expressing CD86 and/or CD69. CD69 expression was particularly evident in the more mature CD23<sup>+</sup> B cell fraction. These cells, however, were unable to secrete autoantibodies in vivo. This is in clear contrast to observations in the anti-DNA Ars/A1 Ig transgenic mice and the MD4xML5 anti-hen egg lysozyme Ig transgenic mice in the presence of soluble lysozyme (Akerlund et al., 2015; Getahun et al., 2016). We reason that these diverging findings are due to the nature and avidity of the self-antigen. In the case of Ars/A1 and MD4xML5 mice, the self-antigen is not membrane bound and reacts with B cells at low avidity. In contrast, the self-antigen in the 3–83Igi,H-2<sup>b</sup> mice is a high-avidity membrane-bound protein that induces robust

internalization of both IgM and IgD BCRs, leaving only 10% on the cell membrane. In both MD4xML5 and 3–83Igi,H-2<sup>b</sup> mice, the protein nature of their self-antigens suggests that T cell help is required to promote effector B cell function. Due to central T cell tolerance, CD4 T cells reactive with K<sup>b</sup> peptides are likely not available to help 3–83Igi<sup>+</sup> B cells in H-2<sup>b</sup> mice. When provided T cell help factors in culture in the form of CD40 and IL-4R signaling, P110\* autoreactive 3–83Igi<sup>+</sup> B cells were able to secrete 3–83 IgM and IgG antibodies. In contrast, our attempts to deliver T cell help in vivo (and by two distinct methods) completely failed to elicit antibody responses. Thus, while active PI3K is able to break peripheral tolerance in low-avidity autoreactive B cells, possibly independently of T cell help, this pathway is unable to break tolerance in high-avidity autoreactive B cells, even in the presence of T cell help. To reconcile our in vitro and in vivo data and our observations in relation to those described for low-avidity autoreactive B cells (Akerlund et al., 2015; Getahun et al., 2016), we consider the following non-mutually exclusive explanations: (1) the production of 3–83 autoantibodies in the anti-CD40\*IL-4 B cell cultures was aided by a dilution of B cells that led to low levels of antigen-mediated BCR stimulation (i.e., low avidity); (2) tolerance in vivo was maintained via a cell population or factor absent in B cell cultures; (3) the lack of productive antibody responses in vivo was caused by diminished CD21 expression on B cells, given this protein contributes to antibody responses (Fearon and Carroll, 2000) and low expression is a sign of exhaustion (Portugal et al., 2017); (4) the lack of antibody response in vivo was caused by the displacement of T cells in follicles and the absence of T<sub>FH</sub> cells; and (5) P110\* was unable to promote high-avidity autoantibodies because, in contrast to P110δ, the P110α isoform does not exhibit full function in mature B cells responding to antigen (Okkenhaug, 2013).

Overall, our study indicates that the PI3K pathway is the master regulator of both negative and positive B cell selection in the bone marrow; low activity in autoreactive cells facilitates receptor editing, while higher activity in nonautoreactive cells halts Ig gene recombination and promotes cell survival, tissue migration, and differentiation. Our data also show that if improperly activated, the PI3K pathway completely abrogates central B cell tolerance, promoting the export of high-avidity autoreactive B cells into the periphery, where they differentiate and undergo activation in response to self-antigen. While it has been shown that activating the PI3K pathway can promote the production of low-avidity autoantibodies (Akerlund et al., 2015; Getahun et al., 2016), here we indicate that high-avidity autoreactive B cells with active PI3K, despite reaching a mature cell stage, remain incapable of secreting autoantibodies. Overall, our findings strongly implicate the PI3K pathway in controlling the primary B cell repertoire and regulating the generation, differentiation, and activation of autoreactive B cells.

## Materials and methods

### Mice

Ig knock-in mice 3–83Igi,H-2<sup>d</sup> (nonautoreactive) and 3–83Igi,H-2<sup>b</sup> (autoreactive) have been previously described (Pelanda et al., 1997; Braun et al., 2000; Halverson et al., 2004; Liu et al., 2005;



Rowland et al., 2010a,b) and were all on a BALB/c genetic background. BALB/c mb1Cre mice (described in Hobeika et al., 2006) were bred to 3-83Igi,H-2<sup>b</sup> and 3-83Igi,H-2<sup>d</sup> mice to generate 3-83Igi,H-2<sup>b</sup> or H-2<sup>d</sup> mb1Cre mice. CB17 mice, bred in-house, were used as wild-type controls. The Rosa26-P110\* mice on a C57BL/6 background have been previously described (Srinivasan et al., 2009). In these mice, a *loxP-stop-loxP* cassette is inserted between the Rosa26 promoter and the P110\* cassette, and an *IRES-GFP* sequence follows P110\*. These features guarantee P110\* and GFP coexpression only in the presence of Cre enzyme. P110\* mice (C57BL/6) were backcrossed to 3-83Igi, H-2<sup>b</sup> or H-2<sup>d</sup> (BALB/c) mice for eight generations and then to the 3-83Igi,H-2<sup>b</sup> or H-2<sup>d</sup> mb1Cre mice to generate autoreactive or nonautoreactive P110\*-mb1Cre mice and mb1Cre littermate controls, respectively. For reasons that remain unclear, 35% of the P110\* 3-83Igi mice on either background were lost before birth, according to Mendelian genetics, and another 10% died at a young age. The bm12 (*H2-Ab1<sup>bm12</sup>*) mice (Morris et al., 1990) were ordered from The Jackson Laboratory (stock 001162). Mice of both sexes were analyzed at 7–9 wk of age. Mice were bred and maintained in a specific pathogen-free facility at the University of Colorado Anschutz Medical Campus Vivarium (Aurora, CO). All animal procedures were approved by the University of Colorado Denver Institutional Animal Care and Use Committee.

#### In vitro immature B cell differentiation

Bone marrow immature B cells were generated and differentiated in vitro as previously described (Rowland et al., 2010a,b; Teodorovic et al., 2014), based on a B cell culture system originally described in Rolink et al. (1995). Briefly, bone marrow cells were cultured in complete IMDM in the presence of IL-7 (made in-house) for 4 d, at which time IL-7 was removed by washing twice with PBS. Then, cells were plated at 6–8 × 10<sup>6</sup> cells/ml with 20 ng/ml recombinant mouse BAFF (R&D Systems) for an additional 2–3 d to achieve cell differentiation (e.g., CD21 expression). Where indicated, cells were treated either DMSO, 5 μM of PI3K inhibitor (LY294002; EMD Millipore), or 5 μM rapamycin (EMD Millipore) during culture with BAFF.

#### In vitro and in vivo B cell stimulation

For in vitro B cell stimulations, splenic B cells were purified by negative selection using anti-CD43 monoclonal antibodies coupled to magnetic beads (Miltenyi Biotech) and an AutoMACS (Miltenyi Biotech) according to the manufacturer's instructions. B cell purity was consistently >95% based on B220 staining. Enriched B cells were cultured at 5 × 10<sup>6</sup> cells/ml with either media alone or with the addition of 15 μg/ml anti-CD40 antibodies (clone IC10) and 50 ng/ml recombinant mouse IL-4. After 7-d incubation, the supernatants were collected and Igs were measured by ELISAs as described below. For the in vivo stimulations with bm12 cells, splenic cells from bm12 mice were depleted of B220<sup>+</sup> cells using anti-B220 antibodies coupled to magnetic beads (Miltenyi Biotech). 25 × 10<sup>6</sup> B220<sup>-</sup> bm12 cells were injected i.v. into each experimental mouse. Mice were bled 14 d after transfer, and serum was collected to measure Igs by ELISAs. For in vivo targeting of CD19, each experimental mouse

was immunized to prime T cells by injecting i.p. 100 μl Alu-Gel-S (Alum) mixed with 150 μg PE. 1 wk after T cell priming, mice were injected with 10 μg PE-conjugated anti-CD19 antibodies (clone 1D3). Mice were bled 14 d after injection, and serum was collected for ELISAs.

#### ELISAs

The 3-83IgM and total IgM serum titers were measured by ELISA as previously described (Liu et al., 2005). The 3-83IgG serum titers were measured by ELISA as previously described (Liu et al., 2005) and with the following modifications. Briefly, 96-well Nunc-Immuno MaxiSorp plates (Thermo Fisher Scientific) were coated with a mixture of rat anti-mouse IgG1 (A85-3), IgG2a (RMG2a-62), IgG2b (RMG2b-1), and IgG3 (R2-38) at a final concentration of 10 μg/ml (all purchased from BioLegend or BD Biosciences). The 3-83IgG was detected using biotinylated anti-3-83Ig antibody (54.1; Nemazee and Bürki, 1989), followed by alkaline phosphatase (AP)-conjugated streptavidin (Southern Biotech), and developed by the addition of AP substrate (p-nitrophenyl phosphate; Sigma). For total IgG ELISA, 96-well Nunc-Immuno MaxiSorp plates were coated with 10 μg/ml of goat anti-mouse IgG (H+L) antibody, human adsorbed (Southern Biotech). Plates were detected with AP-conjugated goat anti-mouse IgG, human adsorbed (Southern Biotech). The standard used to measure total IgG concentration was a mixture of the following mouse unlabeled antibodies starting at 1 μg/ml: IgG1 (15H6), IgG2a (HOPC-1), IgG2b (A-1), IgG3 (B10), all purchased from Southern Biotech. For the Igλ ELISAs, plates were coated with 10 μg/ml unlabeled goat anti-mouse Igλ purchased from Southern Biotech. Plates were detected with AP-conjugated goat anti-mouse Igλ purchased from Southern Biotech. All ELISA plates were developed by the addition of AP substrate (Sigma) solubilized in 0.1 M diethanolamine and 0.02% NaN<sub>3</sub>. Plates were read as previously described (Teodorovic et al., 2012).

#### Quantitative real-time PCR

Ex vivo bone marrow B cells (either B220<sup>+</sup> or B220<sup>+</sup>GFP<sup>+</sup>) were isolated using a FACSARIA (BD Biosciences) cell sorter with a purity of >97%. Total RNA was purified using TRIzol (Invitrogen), and cDNA was synthesized using the SuperScript III First-Strand Synthesis system (Invitrogen). Murine *Rag1* (Mm01270936\_m1), *Rag2* (Mm00501300\_m1), and *FOXO1* (Mm00490671\_m1) cDNAs were amplified using Applied Biosystems TaqMan primer and probe sets purchased from Thermo Fisher Scientific. Differences in specific mRNA levels were determined as previously described (Teodorovic et al., 2014), and each sample was normalized to murine 18s (Mm03928990\_g1, AB TaqMan). All samples were run in triplicate using the QuantStudio 7 Flex Real-Time PCR System (Thermo Fisher Scientific).

#### Flow cytometry

Bone marrow and spleen single-cell suspensions were stained with fluorochrome or biotin-conjugated antibodies against mouse B220 (RA3-6B2), IgD (11-26c-2a), IgM<sup>a</sup> (MA-69), IgM<sup>b</sup> (AF6-78), pan-IgM (11/41), CD21 (7E9), CD23 (B3B4), CD24 (M1/69), CD93 (AA4.1), BAFFR, IL-7R (A7R34), CD43 (1G10), CD2

(RM2-5), Ig $\lambda$  (RML-42), CD19 (1D3), CD138 (281-2), CD86 (B7-2), CD69 (HL2F3), CD1d (1B1), CD44 (1M7), MHC-II I-A/I-E (M5/114.15.2), CD3 (145-2C11), CD4 (GK1.5), CXCR5 (L138D7), and PD-1 (J43) purchased from eBioscience, BD Pharmingen, BioLegend, or R&D Systems. Anti-3-83Ig (H+ $\kappa$ ; 54.1; [Nemazee and Bürki, 1989](#)) and 3-83Ig $\kappa$  (S27; [Liu et al., 2005](#)) antibodies were produced in-house. Biotin-labeled antibodies were visualized with fluorochrome-conjugated streptavidin (BD Biosciences). The fluorescent chemical compound 7-aminoactinomycin D (eBioscience) was used to discriminate unfixed dead cells. pERK, pAKT-S473, pAKT-T308, and FOXO1 (Cell Signaling Technologies) staining was performed on cells permeabilized with methanol. The Zombie UV Fixable Viability kit from BioLegend was used to discriminate dead cells in fixed and permeabilized samples. Data acquisition was done on the CyAn cytometer (Beckman Coulter) or the BD LSRFortessa cytometer (BD Biosciences) and analyzed with FlowJo software (Tree Star). Analyses were performed on live cells based on the incorporation of 7-aminoactinomycin D or Zombie UV or forward and side scatter. B cells were identified by the expression of the pan B cell marker B220. Cell doublets were excluded based on the side scatter and pulse width for data analyzed on the CyAn cytometer or the forward scatter area and forward scatter height for data analyzed on the BD LSRFortessa.

### Histology

Spleens from 3-83Igi, H-2<sup>b</sup> mb1Cre-R26-LSL-P110\*-GFP, 3-83Igi, H-2<sup>b</sup> mb1Cre, 3-83Igi, H-2<sup>d</sup> mb1Cre-R26-LSL-P110\*-GFP, and 3-83Igi, H-2<sup>d</sup> mb1Cre mice were harvested and fixed in a 3% formaldehyde, 3% sucrose solution. The spleens were then frozen at -80°C in OCT compound (EM Sciences), cut into 7- $\mu$ m sections on a cryostat, and transferred onto glass slides. Slides were dried at room temperature (RT) for 30 min. For staining, the slides were rehydrated in PBS for 20 min, blocked with a mixture of anti-mouse CD16 (24G2) Ab, and rat serum in PBS, 2% BSA, and 0.05% Tween20 for 15 min at RT and then stained with antibodies against mouse MOMA-1 (3D6.112), CD3 (145-2C11), and B220 (RA3-6B2) for 45 min at RT in the dark. After three washes in PBS, dried sections were mounted with a coverslip (#1.5 thickness) using Electron Microscopy Science Cytooseal 60 (Fisher Scientific). Sections were visualized on an Eclipse TE 2000 microscope (Nikon) outfitted with a Plan Fluor ELWD Ph2 DM 10 $\times$  objective dry with a 10 $\times$  eyepiece for a total 100 $\times$  magnification. Images were collected using a wide field lens and NIS Elements version 4.2 software and viewed with NIS Elements Viewer version 4.11.0 software (all from Nikon). Fluorochrome settings were set to equivalent intensities among all samples for comparison and analysis. In addition, all files were exported using equivalent settings and file formats.

### Statistical data analysis

Data were analyzed using GraphPad Prism software. Statistical significance for normally distributed data were determined by one-tailed *t* tests, adding the Welch's correction for groups with unequal variance, while data that were not normally distributed were analyzed with the nonparametric Mann-Whitney *U* test. The level of significance was established as follows: \*,  $P < 0.05$ ;

\*\*,  $P < 0.01$ ; \*\*\*,  $P < 0.001$ ; \*\*\*\*,  $P < 0.0001$ ; ns, not significant ( $P > 0.05$ ). Data in graphs are represented as means  $\pm$  SEM.

### Online supplemental material

Fig. S1 shows that B220<sup>-</sup> cells have similar pAKT-T308 levels in P110\* and control mice. It also demonstrates the infrequent expression of GFP/P110\* in B220<sup>+</sup>CD24<sup>-</sup>CD21<sup>-</sup> cells and the increased expression of IL-7R and CR2 transcription in P110\* bone marrow B cells relative to control. Fig. S2 shows that the PI3K inhibitor LY294002, but not rapamycin, inhibits the differentiation of immature B cells into transitional B cells in culture; it also shows the levels of pAKT in bone marrow B cells from MLR/*lpr* mice. Fig. S3 shows the gating strategy of B220<sup>+</sup>GFP<sup>+</sup> and B220<sup>+</sup> B cells in spleen cells from P110\* and control mice, respectively. Fig. S4 indicates the concentration of total IgM, IgG, and Ig $\lambda$  in sera from autoreactive P110\* and control mice. Fig. S5 shows flow cytometric analysis and numbers of T<sub>FH</sub> cells in autoreactive P110\* and control mice and the expression of MHC-II on spleen B cells. It also shows the binding of anti-CD19-PE antibodies to B cells of mice injected with these antibodies and the increase of anti-chromatin Igs in wild-type H-2<sup>b</sup> mice injected with H-2<sup>b</sup>ml2 spleen cells.

### Acknowledgments

We thank Drs. Michael Reth (University of Freiburg and Max Planck Institute of Immunobiology and Epigenetics, Freiburg, Germany) and Jing Wang (University of Colorado, Anschutz Medical Campus, Aurora, CO) for donating mb1Cre and Rosa26-P110\* mice, respectively. We thank the Human Immune Monitoring Shared Resource and ImmunoMicro Flow Facility at the University of Colorado Anschutz Medical Campus for assistance with cell sorting and analysis and the Vivarium at the University of Colorado Anschutz Medical Campus for assistance with mouse husbandry. We are very grateful to all members of our laboratories and to our colleagues Drs. John Cambier and Andy Getahun for the numerous useful discussions.

This work was supported by the National Institute of Health (grants AI052310 and AII31639 to R. Pelanda and grant AII36534 to R.M. Torres). It was also supported in part by the University of Colorado Denver Cancer Center Support Grant P30CA046934 for a shared resource.

The authors declare no competing financial interests.

Author contributions: S.A. Greaves, R. Pelanda, and R.M. Torres contributed to the conception and design of the study; S. A. Greaves and J.N. Peterson performed the experiments. P. Strauch provided significant help with immunofluorescence histology and performed the blind analysis of tissue sections. S. A. Greaves and R. Pelanda analyzed data and drew conclusions. S.A. Greaves wrote the first draft of the manuscript. S.A. Greaves, R. Pelanda, and R.M. Torres contributed to manuscript revision and read and approved the submitted version.

Submitted: 27 August 2018

Revised: 23 January 2019

Accepted: 22 March 2019

## References

- Aiba, Y., M. Kameyama, T. Yamazaki, T.F. Tedder, and T. Kurosaki. 2008. Regulation of B-cell development by BCAP and CD19 through their binding to phosphoinositide 3-kinase. *Blood*. 111:1497–1503. <https://doi.org/10.1182/blood-2007-08-109769>
- Akerlund, J., A. Getahun, and J.C. Cambier. 2015. B cell expression of the SH2-containing inositol 5-phosphatase (SHIP-1) is required to establish anergy to high affinity, proteinacious autoantigens. *J. Autoimmun.* 62: 45–54. <https://doi.org/10.1016/j.jaut.2015.06.007>
- Amin, R.H., and M.S. Schlissel. 2008. Foxo1 directly regulates the transcription of recombination-activating genes during B cell development. *Nat. Immunol.* 9:613–622. <https://doi.org/10.1038/ni.1612>
- Anzelon, A.N., H. Wu, and R.C. Rickert. 2003. Pten inactivation alters peripheral B lymphocyte fate and reconstitutes CD19 function. *Nat. Immunol.* 4:287–294. <https://doi.org/10.1038/ni892>
- Avery, D.T., A. Kane, T. Nguyen, A. Lau, A. Nguyen, H. Lenthall, K. Payne, W. Shi, H. Brigden, E. French, et al. 2018. Germline-activating mutations in PIK3CD compromise B cell development and function. *J. Exp. Med.* 215: 2073–2095. <https://doi.org/10.1084/jem.20180010>
- Bannish, G., E.M. Fuentes-Pananá, J.C. Cambier, W.S. Pear, and J.G. Monroe. 2001. Ligand-independent signaling functions for the B lymphocyte antigen receptor and their role in positive selection during B lymphopoiesis. *J. Exp. Med.* 194:1583–1596. <https://doi.org/10.1084/jem.194.11.1583>
- Baracho, G.V., A.V. Miletic, S.A. Omori, M.H. Cato, and R.C. Rickert. 2011. Emergence of the PI3-kinase pathway as a central modulator of normal and aberrant B cell differentiation. *Curr. Opin. Immunol.* 23:178–183. <https://doi.org/10.1016/j.coi.2011.01.001>
- Beck, T.C., A.C. Gomes, J.G. Cyster, and J.P. Pereira. 2014. CXCR4 and a cell-extrinsic mechanism control immature B lymphocyte egress from bone marrow. *J. Exp. Med.* 211:2567–2581. <https://doi.org/10.1084/jem.20140457>
- Braun, U., K. Rajewsky, and R. Pelanda. 2000. Different sensitivity to receptor editing of B cells from mice hemizygous or homozygous for targeted Ig transgenes. *Proc. Natl. Acad. Sci. USA*. 97:7429–7434. <https://doi.org/10.1073/pnas.050578497>
- Browne, C.D., C.J. Del Nagro, M.H. Cato, H.S. Dengler, and R.C. Rickert. 2009. Suppression of phosphatidylinositol 3,4,5-trisphosphate production is a key determinant of B cell anergy. *Immunity*. 31:749–760. <https://doi.org/10.1016/j.immuni.2009.08.026>
- Cambier, J.C., S.B. Gauld, K.T. Merrell, and B.J. Vilen. 2007. B-cell anergy: from transgenic models to naturally occurring anergic B cells? *Nat. Rev. Immunol.* 7:633–643. <https://doi.org/10.1038/nri2133>
- Cariappa, A., M. Tang, C. Parg, E. Nebelitskiy, M. Carroll, K. Georgopoulos, and S. Pillai. 2001. The follicular versus marginal zone B lymphocyte cell fate decision is regulated by Aiolos, Btk, and CD21. *Immunity*. 14: 603–615. [https://doi.org/10.1016/S1074-7613\(01\)00135-2](https://doi.org/10.1016/S1074-7613(01)00135-2)
- Chen, C., Z. Nagy, M.Z. Radic, R.R. Hardy, D. Huszar, S.A. Camper, and M. Weigert. 1995. The site and stage of anti-DNA B-cell deletion. *Nature*. 373:252–255. <https://doi.org/10.1038/373252a0>
- Chen, J., J.J. Limon, C. Blanc, S.L. Peng, and D.A. Fruman. 2010. Foxo1 regulates marginal zone B-cell development. *Eur. J. Immunol.* 40:1890–1896. <https://doi.org/10.1002/eji.200939817>
- Cheng, S., C.Y. Hsia, B. Feng, M.L. Liou, X. Fang, P.P. Pandolfi, and H.C. Liou. 2009. BCR-mediated apoptosis associated with negative selection of immature B cells is selectively dependent on Pten. *Cell Res.* 19:196–207. <https://doi.org/10.1038/cr.2008.284>
- Corfe, S.A., and C.J. Paige. 2012. The many roles of IL-7 in B cell development; mediator of survival, proliferation and differentiation. *Semin. Immunol.* 24:198–208. <https://doi.org/10.1016/j.smim.2012.02.001>
- Coulter, T.I., A. Chandra, C.M. Bacon, J. Babar, J. Curtis, N. Sreaton, J.R. Goodlad, G. Farmer, C.L. Steele, T.R. Leahy, et al. 2017. Clinical spectrum and features of activated phosphoinositide 3-kinase  $\delta$  syndrome: A large patient cohort study. *J. Allergy Clin. Immunol.* 139:597–606.e4. <https://doi.org/10.1016/j.jaci.2016.06.021>
- Dengler, H.S., G.V. Baracho, S.A. Omori, S. Bruckner, K.C. Arden, D.H. Casttrillon, R.A. DePinho, and R.C. Rickert. 2008. Distinct functions for the transcription factor Foxo1 at various stages of B cell differentiation. *Nat. Immunol.* 9:1388–1398. <https://doi.org/10.1038/ni.1667>
- Diamant, E., Z. Keren, and D. Melamed. 2005. CD19 regulates positive selection and maturation in B lymphopoiesis: lack of CD19 imposes developmental arrest of immature B cells and consequential stimulation of receptor editing. *Blood*. 105:3247–3254. <https://doi.org/10.1182/blood-2004-08-3165>
- Dulau Florea, A.E., R.C. Braylan, K.T. Schafner, K.W. Williams, J. Daub, R.K. Goyal, J.M. Puck, V.K. Rao, S. Pittaluga, S.M. Holland, et al. 2017. Abnormal B-cell maturation in the bone marrow of patients with germline mutations in PIK3CD. *J. Allergy Clin. Immunol.* 139:1032–1035.e6. <https://doi.org/10.1016/j.jaci.2016.08.028>
- Duong, B.H., T. Ota, M. Aoki-Ota, A.B. Cooper, D. Ait-Azzouzene, J.L. Vela, A. L. Gavin, and D. Nemazee. 2011. Negative selection by IgM superantigen defines a B cell central tolerance compartment and reveals mutations allowing escape. *J. Immunol.* 187:5596–5605. <https://doi.org/10.4049/jimmunol.1102479>
- Durand, C.A., K. Hartvigsen, L. Fogelstrand, S. Kim, S. Iritani, B. Vanhaesebroeck, J.L. Witztum, K.D. Puri, and M.R. Gold. 2009. Phosphoinositide 3-kinase p110 delta regulates natural antibody production, marginal zone and B-1 B cell function, and autoantibody responses. *J. Immunol.* 183:5673–5684. <https://doi.org/10.4049/jimmunol.0900432>
- Eisenberg, R.A., and C.S. Via. 2012. T cells, murine chronic graft-versus-host disease and autoimmunity. *J. Autoimmun.* 39:240–247. <https://doi.org/10.1016/j.jaut.2012.05.017>
- Fearon, D.T., and M.C. Carroll. 2000. Regulation of B lymphocyte responses to foreign and self-antigens by the CD19/CD21 complex. *Annu. Rev. Immunol.* 18:393–422. <https://doi.org/10.1146/annurev.immunol.18.1.393>
- Fournier, E.M., M.G. Velez, K. Leahy, C.L. Swanson, A.V. Rubtsov, R.M. Torres, and R. Pelanda. 2012. Dual-reactive B cells are autoreactive and highly enriched in the plasmablast and memory B cell subsets of autoimmune mice. *J. Exp. Med.* 209:1797–1812. <https://doi.org/10.1084/jem.20120332>
- Getahun, A., N.A. Beavers, S.R. Larson, M.J. Shlomchik, and J.C. Cambier. 2016. Continuous inhibitory signaling by both SHP-1 and SHIP-1 pathways is required to maintain unresponsiveness of anergic B cells. *J. Exp. Med.* 213:751–769. <https://doi.org/10.1084/jem.20150537>
- Gonzalez-Martin, A., B.D. Adams, M. Lai, J. Shepherd, M. Salvador-Bernaldez, J.M. Salvador, J. Lu, D. Nemazee, and C. Xiao. 2016. The microRNA miR-148a functions as a critical regulator of B cell tolerance and autoimmunity. *Nat. Immunol.* 17:433–440. <https://doi.org/10.1038/ni.3385>
- Goodnow, C.C., C.G. Vinuesa, K.L. Randall, F. Mackay, and R. Brink. 2010. Control systems and decision making for antibody production. *Nat. Immunol.* 11:681–688. <https://doi.org/10.1038/ni.1900>
- Gorelik, L., A.H. Cutler, G. Thill, S.D. Miklasz, D.E. Shea, C. Ambrose, S.A. Bixler, L. Su, M.L. Scott, and S.L. Kalled. 2004. Cutting edge: BAFF regulates CD21/35 and CD23 expression independent of its B cell survival function. *J. Immunol.* 172:762–766. <https://doi.org/10.4049/jimmunol.172.2.762>
- Grandien, A., R. Fuchs, A. Nobrega, J. Andersson, and A. Coutinho. 1994. Negative selection of multireactive B cell clones in normal adult mice. *Eur. J. Immunol.* 24:1345–1352. <https://doi.org/10.1002/eji.1830240616>
- Greaves, S.A., J.N. Peterson, R.M. Torres, and R. Pelanda. 2018. Activation of the MEK-ERK Pathway Is Necessary but Not Sufficient for Breaking Central B Cell Tolerance. *Front. Immunol.* 9:707. <https://doi.org/10.3389/fimmu.2018.00707>
- Halverson, R., R.M. Torres, and R. Pelanda. 2004. Receptor editing is the main mechanism of B cell tolerance toward membrane antigens. *Nat. Immunol.* 5:645–650. <https://doi.org/10.1038/ni1076>
- Hardy, R.R., C.E. Carmack, S.A. Shinton, J.D. Kemp, and K. Hayakawa. 2012. Resolution and characterization of pro-B and pre-pro-B cell stages in normal mouse bone marrow. 1991. *J. Immunol.* 189:3271–3283.
- Herzog, S., E. Hug, S. Meixlsperger, J.H. Paik, R.A. DePinho, M. Reth, and H. Jumaa. 2008. SLP-65 regulates immunoglobulin light chain gene recombination through the PI(3)K-PKB-Foxo pathway. *Nat. Immunol.* 9: 623–631. <https://doi.org/10.1038/ni.1616>
- Hobeika, E., S. Thiemann, B. Storch, H. Jumaa, P.J. Nielsen, R. Pelanda, and M. Reth. 2006. Testing gene function early in the B cell lineage in mb1-cre mice. *Proc. Natl. Acad. Sci. USA*. 103:13789–13794. <https://doi.org/10.1073/pnas.0605944103>
- Hsu, B.L., S.M. Harless, R.C. Lindsley, D.M. Hilbert, and M.P. Cancro. 2002. Cutting edge: BLYS enables survival of transitional and mature B cells through distinct mediators. *J. Immunol.* 168:5993–5996. <https://doi.org/10.4049/jimmunol.168.12.5993>
- Kinnunen, T., N. Chamberlain, H. Morbach, T. Cantaert, M. Lynch, P. Preston-Hurlburt, K.C. Herold, D.A. Hafler, K.C. O'Connor, and E. Meffre. 2013. Specific peripheral B cell tolerance defects in patients with multiple sclerosis. *J. Clin. Invest.* 123:2737–2741. <https://doi.org/10.1172/JCI68775>
- Klippel, A., C. Reinhard, W.M. Kavanaugh, G. Apell, M.A. Escobedo, and L.T. Williams. 1996. Membrane localization of phosphatidylinositol 3-kinase is sufficient to activate multiple signal-transducing kinase pathways. *Mol. Cell. Biol.* 16:4117–4127. <https://doi.org/10.1128/MCB.16.8.4117>



- Kouskoff, V., G. Lacaud, K. Pape, M. Retter, and D. Nemazee. 2000. B cell receptor expression level determines the fate of developing B lymphocytes: receptor editing versus selection. *Proc. Natl. Acad. Sci. USA*. 97: 7435–7439. <https://doi.org/10.1073/pnas.130182597>
- Kövesdi, D., S.E. Bell, and M. Turner. 2010. The development of mature B lymphocytes requires the combined function of CD19 and the p110 $\delta$  subunit of PI3K. *Self Nonself*. 1:144–153. <https://doi.org/10.4161/self.1.2.11796>
- Kraus, M., M.B. Alimzhanov, N. Rajewsky, and K. Rajewsky. 2004. Survival of resting mature B lymphocytes depends on BCR signaling via the Ig-alpha/beta heterodimer. *Cell*. 117:787–800. <https://doi.org/10.1016/j.cell.2004.05.014>
- Lam, K.P., R. Kühn, and K. Rajewsky. 1997. In vivo ablation of surface immunoglobulin on mature B cells by inducible gene targeting results in rapid cell death. *Cell*. 90:1073–1083. [https://doi.org/10.1016/S0092-8674\(00\)80373-6](https://doi.org/10.1016/S0092-8674(00)80373-6)
- Lamoureaux, J.L., L.C. Watson, M. Cherrier, P. Skog, D. Nemazee, and A.J. Feeney. 2007. Reduced receptor editing in lupus-prone MRL/lpr mice. *J. Exp. Med.* 204:2853–2864. <https://doi.org/10.1084/jem.20071268>
- Lang, J., M. Jackson, L. Teyton, A. Brunmark, K. Kane, and D. Nemazee. 1996. B cells are exquisitely sensitive to central tolerance and receptor editing induced by ultralow affinity, membrane-bound antigen. *J. Exp. Med.* 184:1685–1697. <https://doi.org/10.1084/jem.184.5.1685>
- Lang, J., T. Ota, M. Kelly, P. Strauch, B.M. Freed, R.M. Torres, D. Nemazee, and R. Pelanda. 2016. Receptor editing and genetic variability in human autoreactive B cells. *J. Exp. Med.* 213:93–108. <https://doi.org/10.1084/jem.20151039>
- Lazorchak, A.S., D. Liu, V. Facchinetti, A. Di Lorenzo, W.C. Sessa, D.G. Schatz, and B. Su. 2010. Sin1-mTORC2 suppresses rag and il7r gene expression through Akt2 in B cells. *Mol. Cell*. 39:433–443. <https://doi.org/10.1016/j.molcel.2010.07.031>
- Leung, W.H., T. Tarasenko, Z. Biesova, H. Kole, E.R. Walsh, and S. Bolland. 2013. Aberrant antibody affinity selection in SHIP-deficient B cells. *Eur. J. Immunol.* 43:371–381. <https://doi.org/10.1002/eji.201242809>
- Li, Y., H. Li, and M. Weigert. 2002. Autoreactive B cells in the marginal zone that express dual receptors. *J. Exp. Med.* 195:181–188. <https://doi.org/10.1084/jem.20011453>
- Limon, J.J., and D.A. Fruman. 2012. Akt and mTOR in B Cell Activation and Differentiation. *Front. Immunol.* 3:228. <https://doi.org/10.3389/fimmu.2012.00228>
- Lindsley, R.C., M. Thomas, B. Srivastava, and D. Allman. 2007. Generation of peripheral B cells occurs via two spatially and temporally distinct pathways. *Blood*. 109:2521–2528. <https://doi.org/10.1182/blood-2006-04-018085>
- Liu, Q., A.J. Oliveira-Dos-Santos, S. Mariathasan, D. Bouchard, J. Jones, R. Sarao, I. Kozieradzki, P.S. Ohashi, J.M. Penninger, and D.J. Dumont. 1998. The inositol polyphosphate 5-phosphatase ship is a crucial negative regulator of B cell antigen receptor signaling. *J. Exp. Med.* 188: 1333–1342. <https://doi.org/10.1084/jem.188.7.1333>
- Liu, S., M.G. Velez, J. Humann, S. Rowland, F.J. Conrad, R. Halverson, R.M. Torres, and R. Pelanda. 2005. Receptor editing can lead to allelic inclusion and development of B cells that retain antibodies reacting with high avidity autoantigens. *J. Immunol.* 175:5067–5076. <https://doi.org/10.4049/jimmunol.175.8.5067>
- Llorian, M., Z. Stamataki, S. Hill, M. Turner, and I.L. Mårtensson. 2007. The PI3K p110delta is required for down-regulation of RAG expression in immature B cells. *J. Immunol.* 178:1981–1985. <https://doi.org/10.4049/jimmunol.178.4.1981>
- Loder, F., B. Mutschler, R.J. Ray, C.J. Paige, P. Sideras, R. Torres, M.C. Lamers, and R. Carsetti. 1999. B cell development in the spleen takes place in discrete steps and is determined by the quality of B cell receptor-derived signals. *J. Exp. Med.* 190:75–89. <https://doi.org/10.1084/jem.190.1.75>
- Ma, Y., D. Xiang, J. Sun, C. Ding, M. Liu, X. Hu, G. Li, G. Kloecker, H.G. Zhang, and J. Yan. 2013. Targeting of antigens to B lymphocytes via CD19 as a means for tumor vaccine development. *J. Immunol.* 190:5588–5599. <https://doi.org/10.4049/jimmunol.1203216>
- Manning, B.D., and A. Toker. 2017. AKT/PKB Signaling: Navigating the Network. *Cell*. 169:381–405. <https://doi.org/10.1016/j.cell.2017.04.001>
- Meffre, E. 2011. The establishment of early B cell tolerance in humans: lessons from primary immunodeficiency diseases. *Ann. N. Y. Acad. Sci.* 1246: 1–10. <https://doi.org/10.1111/j.1749-6632.2011.06347.x>
- Monroe, J.G. 2006. ITAM-mediated tonic signalling through pre-BCR and BCR complexes. *Nat. Rev. Immunol.* 6:283–294. <https://doi.org/10.1038/nri1808>
- Morris, S.C., P.L. Cohen, and R.A. Eisenberg. 1990. Experimental induction of systemic lupus erythematosus by recognition of foreign Ia. *Clin. Immunol. Immunopathol.* 57:263–273. [https://doi.org/10.1016/0090-1229\(90\)90040-W](https://doi.org/10.1016/0090-1229(90)90040-W)
- Nemazee, D. 2006. Receptor editing in lymphocyte development and central tolerance. *Nat. Rev. Immunol.* 6:728–740. <https://doi.org/10.1038/nri1939>
- Nemazee, D.A., and K. Bürki. 1989. Clonal deletion of B lymphocytes in a transgenic mouse bearing anti-MHC class I antibody genes. *Nature*. 337: 562–566. <https://doi.org/10.1038/337562a0>
- Okkenhaug, K. 2013. Signaling by the phosphoinositide 3-kinase family in immune cells. *Annu. Rev. Immunol.* 31:675–704. <https://doi.org/10.1146/annurev-immunol-032712-095946>
- Okkenhaug, K., and B. Vanhaesebroeck. 2003. PI3K in lymphocyte development, differentiation and activation. *Nat. Rev. Immunol.* 3:317–330. <https://doi.org/10.1038/nri1056>
- Okkenhaug, K., A. Bilancio, G. Farjot, H. Priddle, S. Sancho, E. Peskett, W. Pearce, S.E. Meek, A. Salpekar, M.D. Waterfield, et al. 2002. Impaired B and T cell antigen receptor signaling in p110delta PI 3-kinase mutant mice. *Science*. 297:1031–1034.
- Otero, D.C., and R.C. Rickert. 2003. CD19 function in early and late B cell development. II. CD19 facilitates the pro-B/pre-B transition. *J. Immunol.* 171:5921–5930. <https://doi.org/10.4049/jimmunol.171.11.5921>
- Otero, D.C., S.A. Omori, and R.C. Rickert. 2001. Cd19-dependent activation of Akt kinase in B-lymphocytes. *J. Biol. Chem.* 276:1474–1478. <https://doi.org/10.1074/jbc.M003918200>
- Otero, D.C., A.N. Anzelon, and R.C. Rickert. 2003. CD19 function in early and late B cell development: I. Maintenance of follicular and marginal zone B cells requires CD19-dependent survival signals. *J. Immunol.* 170:73–83. <https://doi.org/10.4049/jimmunol.170.1.73>
- Pelanda, R., and R.M. Torres. 2006. Receptor editing for better or for worse. *Curr. Opin. Immunol.* 18:184–190. <https://doi.org/10.1016/j.coi.2006.01.005>
- Pelanda, R., and R.M. Torres. 2012. Central B-cell tolerance: where selection begins. *Cold Spring Harb. Perspect. Biol.* 4:a007146. <https://doi.org/10.1101/cshperspect.a007146>
- Pelanda, R., S. Schwes, E. Sonoda, R.M. Torres, D. Nemazee, and K. Rajewsky. 1997. Receptor editing in a transgenic mouse model: site, efficiency, and role in B cell tolerance and antibody diversification. *Immunity*. 7: 765–775. [https://doi.org/10.1016/S1074-7613\(00\)80395-7](https://doi.org/10.1016/S1074-7613(00)80395-7)
- Portugal, S., N. Obeng-Adjei, S. Moir, P.D. Crompton, and S.K. Pierce. 2017. Atypical memory B cells in human chronic infectious diseases: An intertypical report. *Cell. Immunol.* 321:18–25. <https://doi.org/10.1016/j.cellimm.2017.07.003>
- Preite, S., J.L. Cannons, A.J. Radtke, I. Vujkovic-Cvijin, J. Gomez-Rodriguez, S. Volpi, B. Huang, J. Cheng, N. Collins, J. Reilly, et al. 2018. Hyperactivated PI3K $\delta$  promotes self and commensal reactivity at the expense of optimal humoral immunity. *Nat. Immunol.* 19:986–1000. <https://doi.org/10.1038/s41590-018-0182-3>
- Rajalingam, K., R. Schreck, U.R. Rapp, and S. Albert. 2007. Ras oncogenes and their downstream targets. *Biochim. Biophys. Acta*. 1773:1177–1195. <https://doi.org/10.1016/j.bbamcr.2007.01.012>
- Ramadani, F., D.J. Bolland, F. Garcon, J.L. Emery, B. Vanhaesebroeck, A.E. Corcoran, and K. Okkenhaug. 2010. The PI3K isoforms p110alpha and p110delta are essential for pre-B cell receptor signaling and B cell development. *Sci. Signal.* 3:ra60. <https://doi.org/10.1126/scisignal.2001104>
- Rolink, A., P. Ghia, U. Grawunder, D. Haasner, H. Karasuyama, C. Kalberer, T. Winkler, and F. Melchers. 1995. In-vitro analyses of mechanisms of B-cell development. *Semin. Immunol.* 7:155–167. [https://doi.org/10.1016/1044-5323\(95\)90043-8](https://doi.org/10.1016/1044-5323(95)90043-8)
- Roskoski, R. Jr. 2012. ERK1/2 MAP kinases: structure, function, and regulation. *Pharmacol. Res.* 66:105–143. <https://doi.org/10.1016/j.phrs.2012.04.005>
- Rowland, S.L., C.L. DePersis, R.M. Torres, and R. Pelanda. 2010a. Ras activation of Erk restores impaired tonic BCR signaling and rescues immature B cell differentiation. *J. Exp. Med.* 207:607–621. <https://doi.org/10.1084/jem.20091673>
- Rowland, S.L., K.F. Leahy, R. Halverson, R.M. Torres, and R. Pelanda. 2010b. BAFF receptor signaling aids the differentiation of immature B cells into transitional B cells following tonic BCR signaling. *J. Immunol.* 185: 4570–4581. <https://doi.org/10.4049/jimmunol.1001708>
- Samuels, J., Y.S. Ng, C. Coupillaud, D. Paget, and E. Meffre. 2005. Impaired early B cell tolerance in patients with rheumatoid arthritis. *J. Exp. Med.* 201:1659–1667. <https://doi.org/10.1084/jem.20042321>
- Sasaki, Y., S. Casola, J.L. Kutok, K. Rajewsky, and M. Schmidt-Supprian. 2004. TNF family member B cell-activating factor (BAFF)

- receptor-dependent and -independent roles for BAFF in B cell physiology. *J. Immunol.* 173:2245–2252. <https://doi.org/10.4049/jimmunol.173.4.2245>
- Shojaee, S., L.N. Chan, M. Buchner, V. Cazzaniga, K.N. Cosgun, H. Geng, Y.H. Qiu, M.D. von Minden, T. Ernst, A. Hochhaus, et al. 2016. PTEN opposes negative selection and enables oncogenic transformation of pre-B cells. *Nat. Med.* 22:379–387. <https://doi.org/10.1038/nm.4062>
- So, L., S.S. Yea, J.S. Oak, M. Lu, A. Manmadhan, Q.H. Ke, M.R. Janes, L.V. Kessler, J.M. Kucharski, L.S. Li, et al. 2013. Selective inhibition of phosphoinositide 3-kinase p110 $\alpha$  preserves lymphocyte function. *J. Biol. Chem.* 288:5718–5731. <https://doi.org/10.1074/jbc.M112.379446>
- Srinivasan, L., Y. Sasaki, D.P. Calado, B. Zhang, J.H. Paik, R.A. DePinho, J.L. Kutok, J.F. Kearney, K.L. Otipoby, and K. Rajewsky. 2009. PI3 kinase signals BCR-dependent mature B cell survival. *Cell.* 139:573–586. <https://doi.org/10.1016/j.cell.2009.08.041>
- Srivastava, B., W.J. Quinn III, K. Hazard, J. Erikson, and D. Allman. 2005. Characterization of marginal zone B cell precursors. *J. Exp. Med.* 202:1225–1234. <https://doi.org/10.1084/jem.20051038>
- Suárez-Fueyo, A., D.F. Barber, J. Martínez-Ara, A.C. Zea-Mendoza, and A.C. Carrera. 2011. Enhanced phosphoinositide 3-kinase  $\delta$  activity is a frequent event in systemic lupus erythematosus that confers resistance to activation-induced T cell death. *J. Immunol.* 187:2376–2385. <https://doi.org/10.4049/jimmunol.1101602>
- Suzuki, A., T. Kaisho, M. Ohishi, M. Tsukio-Yamaguchi, T. Tsubata, P.A. Koni, T. Sasaki, T.W. Mak, and T. Nakano. 2003. Critical roles of Pten in B cell homeostasis and immunoglobulin class switch recombination. *J. Exp. Med.* 197:657–667. <https://doi.org/10.1084/jem.20021101>
- Teodorovic, L.S., C. Riccardi, R.M. Torres, and R. Pelanda. 2012. Murine B cell development and antibody responses to model antigens are not impaired in the absence of the TNF receptor GITR. *PLoS One.* 7:e31632. <https://doi.org/10.1371/journal.pone.0031632>
- Teodorovic, L.S., C. Babolin, S.L. Rowland, S.A. Greaves, D.P. Baldwin, R.M. Torres, and R. Pelanda. 2014. Activation of Ras overcomes B-cell tolerance to promote differentiation of autoreactive B cells and production of autoantibodies. *Proc. Natl. Acad. Sci. USA.* 111:E2797–E2806. <https://doi.org/10.1073/pnas.1402159111>
- Tipton, C.M., C.F. Fucile, J. Darce, A. Chida, T. Ichikawa, I. Gregoret, S. Schieferl, J. Hom, S. Jenks, R.J. Feldman, et al. 2015. Diversity, cellular origin and autoreactivity of antibody-secreting cell population expansions in acute systemic lupus erythematosus. *Nat. Immunol.* 16:755–765. <https://doi.org/10.1038/ni.3175>
- Tze, L.E., B.R. Schram, K.P. Lam, K.A. Hogquist, K.L. Hippen, J. Liu, S.A. Shinton, K.L. Otipoby, P.R. Rodine, A.L. Vegoe, et al. 2005. Basal immunoglobulin signaling actively maintains developmental stage in immature B cells. *PLoS Biol.* 3:e82. <https://doi.org/10.1371/journal.pbio.0030082>
- Verkoczy, L., D. Ait-Azzouzene, P. Skog, A. Mårtensson, J. Lang, B. Duong, and D. Nemazee. 2005. A role for nuclear factor kappa B/rel transcription factors in the regulation of the recombinase activator genes. *Immunity.* 22:519–531. <https://doi.org/10.1016/j.immuni.2005.03.006>
- Verkoczy, L., B. Duong, P. Skog, D. Ait-Azzouzene, K. Puri, J.L. Vela, and D. Nemazee. 2007. Basal B cell receptor-directed phosphatidylinositol 3-kinase signaling turns off RAGs and promotes B cell-positive selection. *J. Immunol.* 178:6332–6341. <https://doi.org/10.4049/jimmunol.178.10.6332>
- Wardemann, H., S. Yurasov, A. Schaefer, J.W. Young, E. Meffre, and M.C. Nussenzweig. 2003. Predominant autoantibody production by early human B cell precursors. *Science.* 301:1374–1377. <https://doi.org/10.1126/science.1086907>
- Wen, L., J. Brill-Dashoff, S.A. Shinton, M. Asano, R.R. Hardy, and K. Hayakawa. 2005. Evidence of marginal-zone B cell-positive selection in spleen. *Immunity.* 23:297–308. <https://doi.org/10.1016/j.immuni.2005.08.007>
- Wray-Dutra, M.N., F. Al Qureshah, G. Metzler, M. Oukka, R.G. James, and D.J. Rawlings. 2018. Activated PI3KCD drives innate B cell expansion yet limits B cell-intrinsic immune responses. *J. Exp. Med.* 215:2485–2496. <https://doi.org/10.1084/jem.20180617>
- Wu, T., X. Qin, Z. Kurepa, K.R. Kumar, K. Liu, H. Kanta, X.J. Zhou, A.B. Satterthwaite, L.S. Davis, and C. Mohan. 2007. Shared signaling networks active in B cells isolated from genetically distinct mouse models of lupus. *J. Clin. Invest.* 117:2186–2196. <https://doi.org/10.1172/JCI30398>
- Yan, J., M.J. Wolff, J. Unternehrer, I. Mellman, and M.J. Mamula. 2005. Targeting antigen to CD19 on B cells efficiently activates T cells. *Int. Immunol.* 17:869–877. <https://doi.org/10.1093/intimm/dxh266>
- Yurasov, S., H. Wardemann, J. Hammersen, M. Tsuiji, E. Meffre, V. Pascual, and M.C. Nussenzweig. 2005. Defective B cell tolerance checkpoints in systemic lupus erythematosus. *J. Exp. Med.* 201:703–711. <https://doi.org/10.1084/jem.20042251>